4-2-2015

A Tale of Two Projects: Basis for Centrosome Amplification after DNA Damage and Practical Assessment of Photodamage in Live-Cell Imaging: A Dissertation

Stephen Douthwright
University of Massachusetts Medical School

A TALE OF TWO PROJECTS: BASIS FOR CENTROSOME AMPLIFICATION AFTER DNA DAMAGE AND PRACTICAL ASSESSMENT OF PHOTODAMAGE IN LIVE-CELL IMAGING

A Dissertation Presented

By

Stephen Roy Douthwright

Submitted to the faculty of the
University of Massachusetts Graduate School of Biomedical Sciences, Worcester
in partial fulfillment of the requirement for the degree of

DOCTOR OF PHILOSOPHY

April 2nd, 2015

Interdisciplinary Graduate Program

A TALE OF TWO PROJECTS: BASIS FOR CENTROSOME AMPLIFICATION AFTER DNA DAMAGE AND PRACTICAL ASSESSMENT OF PHOTODAMAGE IN LIVE-CELL IMAGING

A Dissertation Presented
By
Stephen Roy Douthwright

The signatures of the Dissertation Defense Committee signify completion and approval as to style and content of the Dissertation

_____
Greenfield Sluder, Ph.D., Thesis Advisor

_____
Nicholas Rhind, Ph.D., Member of Committee

_____
Michael Sanderson, Ph.D., Member of Committee

_____
William Theurkauf, Ph.D., Member of Committee

_____
Edward Hinchcliffe, Ph.D., Member of Committee

The signature of the Chair of the Committee signifies that the written dissertation meets the requirements of the Dissertation Committee

_____
Dannel McCollum, PhD, Chair of Committee

The signature of the Dean of the Graduate School of Biomedical Sciences signifies that the student has met all graduation requirements of the School

_____
Anthony Carruthers, Ph.D.
Dean of the Graduate School of Biomedical Sciences

Interdisciplinary Graduate Program
April 2nd, 2015

I dedicate this work to my loving wife Catherine and my family
for all of their support and encouragement
over the past six years

Thank you!

ACKNOWLEDGEMENTS

I owe great gratitude to many people for their assistance and guidance throughout the course of my PhD career. First, I'd like to thank my advisor and mentor, Dr. Greenfield (Kip) Sluder. During my time Kip not only introduced me to the wonderful world of microscopy, but he helped me grow tremendously as a scientist. He allowed the freedom to think creatively about my projects, but ensured I always focused on the big picture. While frustrating at times, Kip never gave me an easy answer to any question. This forced me to dedicate much thought into everything I did which truly led to my development as an independent researcher.

I would also like to thank all of past and present members of the Sluder Lab, who each had a role during my time here. Josh Nordberg, the senior graduate student when I started, who I constantly bugged to teach me everything he knew about microscopy, but also provided me great advice on graduate school. Toshi Hatano for all the helpful scientific discussions as well as much needed laughter during his time here. Anna Krzywicka-Racka and Yumi Uetake for their amazing mentorship as senior members of the lab. Much of what I learned during my time is due to the both of you.

For their mentoring and guidance throughout the years I would like to thank the members of my thesis advisory committee: Dr. Dannel McCollum, Dr. Nicholas Rhind, Dr. Mike Sanderson, and Dr. William Theurkauf. I would also like to thank Dr. Kirsten Hagstrom for serving on my qualifying exam committee.

Additionally, I would like to thank Dr. Kendall Knight who took me into his lab as an undergraduate and sparked my interest in research and also provided me much support while a graduate student. I would also like to think Dr. Hinchcliffe for being a part of my dissertation examination committee. Your time is very much appreciated.

I would like to thank my friends here at graduate school for all the great memories, road trips, and thorough discussions about science. You instilled the fun graduate school needed and your friendship is forever appreciated.

Last but not least, I would like to thank my family. My wife Catherine, whom I met in graduate school, for all of her love, patience, and support over the years. Being able to vent to someone who knew exactly how frustrating school can be meant the world to me. My mother and father, who have always encouraged and supported me during graduate school, through good times and bad. Thank you for always showing a strong interest in my work and listening to me carry on about science. My sister who was always the first person to wish me good luck before a talk or meeting and the first to ask how they went. Your love and support helped carry me through this journey.

My deepest thanks to every one of you!!!

ABSTRACT

This thesis comprises two separate studies that focus on the consequences of cellular damage. The first investigates the effects of DNA damage on centriole behavior and the second characterizes phototoxicity during live-cell imaging.

Cancer treatments such as ionizing radiation and/or chemotherapeutic DNA damaging agents are intended to kill tumor cells, but they also damage normal proliferating cells. Although centrosome amplification after DNA damage is a well-established phenomenon for transformed cells, it is not fully understood in untransformed cells. The presence of extra centrosomes in normal cell populations raises the chances of genomic instability, thus posing additional threats to patients undergoing these therapies. I characterized centriole behavior after DNA damage in synchronized untransformed (RPE1) human cells. Treatment with the radiomimetic drug, Doxorubicin, prolongs G2 phase by at least 72hrs, where 52% of cells display disengaged centrioles and 10% contain extra centrioles. This disengagement is mediated by Plk and APC/C activities both singly and in combination. Disengaged centrioles are associated with maturation markers suggesting they are capable of organizing spindle poles. Despite the high incidence of centriole disengagement, only a small percentage of centrioles reduplicate due to p53/p21 dependent inhibition of Cdk2 activity. Although all cells become prolonged in G2 phase, 14% eventually go through mitosis, of which 26% contain disengaged or extra centrioles.

In addition to cancer treatments, cellular damage can be acquired from various external conditions. Short wavelengths of light are known to be toxic to living cells, but are commonly used during live-cell microscopy to excite fluorescent proteins. I characterized the phototoxic effects of blue (488nm) and green (546nm) light on cell cycle progression in RPE1. For unlabeled cells, I found that exposure to green light is far less toxic than blue light, but is not benign. However, the presence of fluorescent proteins led to increased sensitivity to both blue and green light. For 488nm irradiations, spreading the total irradiation durations out into a series of 10s pulses or conducting single longer, but lower intensity, exposures made no significant changes in phototoxicity. However, reducing oxidative stress by culturing cells at physiological (~3%) oxygen, or treatment with a water-soluble antioxidant, Trolox, greatly improved the cells tolerance to blue light.

Collectively, my work offers an explanation for centrosome amplification after DNA damage and demonstrates the importance of proper centriole regulation in untransformed human cells. Further, it provides a practical assessment of photodamage during live-cell imaging.

TABLE OF CONTENTS

LIST OF TABLES

LIST OF FIGURES

LIST OF THIRD PARTY COPYRIGHTED MATERIAL

The following material was reproduced from published work:

	Publisher	License number
Figure I-3	Elsevier	3586171274717
Chapter II	John Wiley and Sons	3586170551378
Figure I-1	Korean Society for Molecular and Cellular Biology	No number needed

The following material was reproduced from published work with no permission required:

	Publisher
Figure I-2	Biomed Central

LIST OF ABBREVIATIONS

MTOC – Microtubule-Organizing Center

PCM – Pericentriolar Material

RPE1 – Retina Pigment Epithelial Cell Line

Plk– Polo Like Kinase

APC/C – Anaphase Promoting Complex/Cyclosome

Cdk – Cyclin Dependent Kinase

U2OS – Human Osteosarcoma Cell Line

HeLa – Human Cervical Cancer Cell Line

RO-3306 – Cdk1 inhibitor

BI 2536 – Plk inhibitor

proTAME – APC/C inhibitor

ROS – Reactive Oxygen Species

OD—Optical Density

PREFACE

Parts of this dissertation appeared in:

Douthwright, S and Sluder, G. 2014. Link Between DNA Damage and Centriole Disengagement/Reduplication in Untransformed Human Cells. J Cell Phys 229(10):1427-36.

CHAPTER I: INTRODUCTION

Centrosome Structure and Function

The centrosome is an organelle that serves as the primary microtubule-organizing center (MTOC) in mammalian cells and has a strong influence on microtubule-dependent processes. During interphase, these effects include cell polarity, cell shape, cell motility, and organelle transport. Further, in certain somatic cells the centrosome moves to the cell cortex, where the older, or mother, centriole becomes the basal body, which initiates the assembly of cilia and flagella (reviewed in Loncarek and Khodjakov, 2009).

The interphase centrosome consists of two orthogonally arranged cylindrical structures called centrioles. The walls of centrioles in higher eukaryotes are made up of nine microtubule triplets, composed of alpha and beta tubulin, surrounding a central pinwheel shaped core. Structurally, the older (mother centriole) is distinguished from the newer (daughter centriole) by the presence of distal and sub-distal appendages, which are responsible for attaching the centriole to the plasma membrane during ciliogenesis and anchoring of microtubules, respectively. Surrounding the centrioles is an electron-dense material known as the pericentriolar material (PCM). The PCM consists of many protein complexes responsible for nucleation and organization of both interphase and mitotic microtubules. Most notably the gamma-tubulin

ring complexes act as templates for microtubule nucleation within the PCM. While the PCM is known to be important for microtubule nucleation, recent studies have also suggested the size of the PCM could play a role in controlling the number of centrioles formed in the centrosome (Loncarek et al, 2008). For a diagram of centrosome structure see **figure I-1**.

Although centrosomes have roles during interphase, arguably, the most important functions of centrosomes are during mitosis. By the start of mitosis the cell contains two pairs of centrosomes. After nuclear envelope breakdown the two pairs of centrosomes separate to form the two poles of the spindle. At this time, the centrosomes nucleate microtubules responsible for interacting with kinetochores to help ensure equal segregation of chromosomes (Rieder and Salmon, 1998). Centrosomes also nucleate astral microtubules which interact with the cell cortex, and in doing so, centrosomes act in a dominant fashion in determining spindle polarity, position, and orientation (reviewed in Hinchcliffe and Sluder, 2001). Interestingly, cells lacking centrosomes can still progress through mitosis and form bipolar spindles through dynein mediated organization of microtubules (Hornick et al., 2011). However, acentrosomal microtubule arrays lack astral microtubules, and thus, encounter problems during cytokinesis due to defects in spindle positioning (Khodjakov and Reider, 2001).

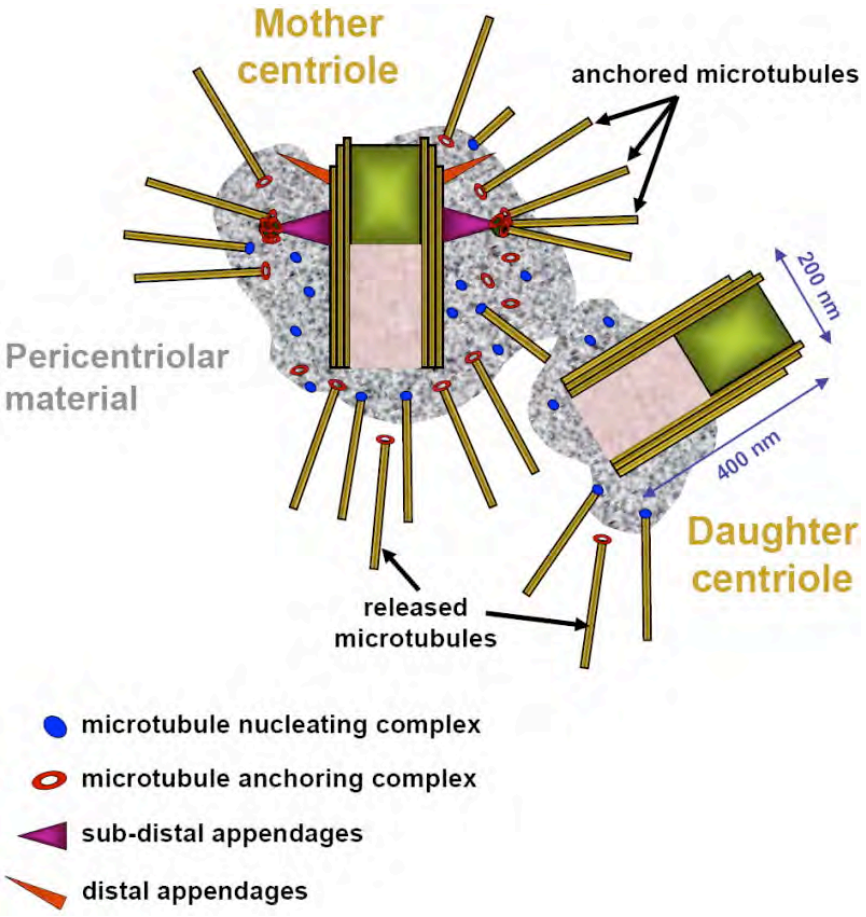

Figure I-1. Centrosome Structure. The centrosome consists of two centrioles, an "older" mother and a "younger" daughter, that are embedded in clouds of pericentriolar matter. The walls of each centriole are made up of nine microtubule triplets. The mother centriole contains two sets of appendages on the outer wall that the daughter lacks. The distal appendages are responsible for attaching the centriole to the plasma membrane during ciliogenesis, while the sub-distal appendages anchor microtubule minus ends. The pericentriolar material surrounding both centrioles contains proteins responsible for microtubule nucleation and anchoring. While microtubules can be nucleated in the PCM present around the daughter centriole, they cannot anchor and are released. This figure is reproduced from Loncarek and Khodjakov, 2009 with permission from the Korean Society of Molecular and Cellular Biology

Centrosome Duplication Cycle

To ensure the cell forms a bipolar spindle there must be two pairs of centrosomes by the start of mitosis. To accomplish this, centrosomes go through a duplication cycle, similar to that of DNA, with each process initiated with a rise in CDK2/E activity (reviewed in Hinchcliffe and Sluder, 2002). For a diagrammatic overview of the centrosome duplication cycle please see **figure I-2**.

Centrosome duplication is believed to begin in late mitosis or early G1, when the centrioles inherited at the end of mitosis become disengaged and lose their orthogonal orientation. Recent studies have suggested that the combined activities of Plk1 and Separase play a major role in centriole disengagement, although the exact mechanism remains unknown (Tsou and Stearns, 2006; Tsou et al., 2009). This disengagement of centrioles is believed to be the "licensing step", which is required before they can duplicate. As the cell progresses into S-phase, a short procentriole forms adjacent to each parental centriole at the proximal ends, where it remains engaged until the following G1. The presence of this daughter centriole is believed to block the mother from producing more than one centriole during this time. Exactly how these procentrioles form still remains unclear.

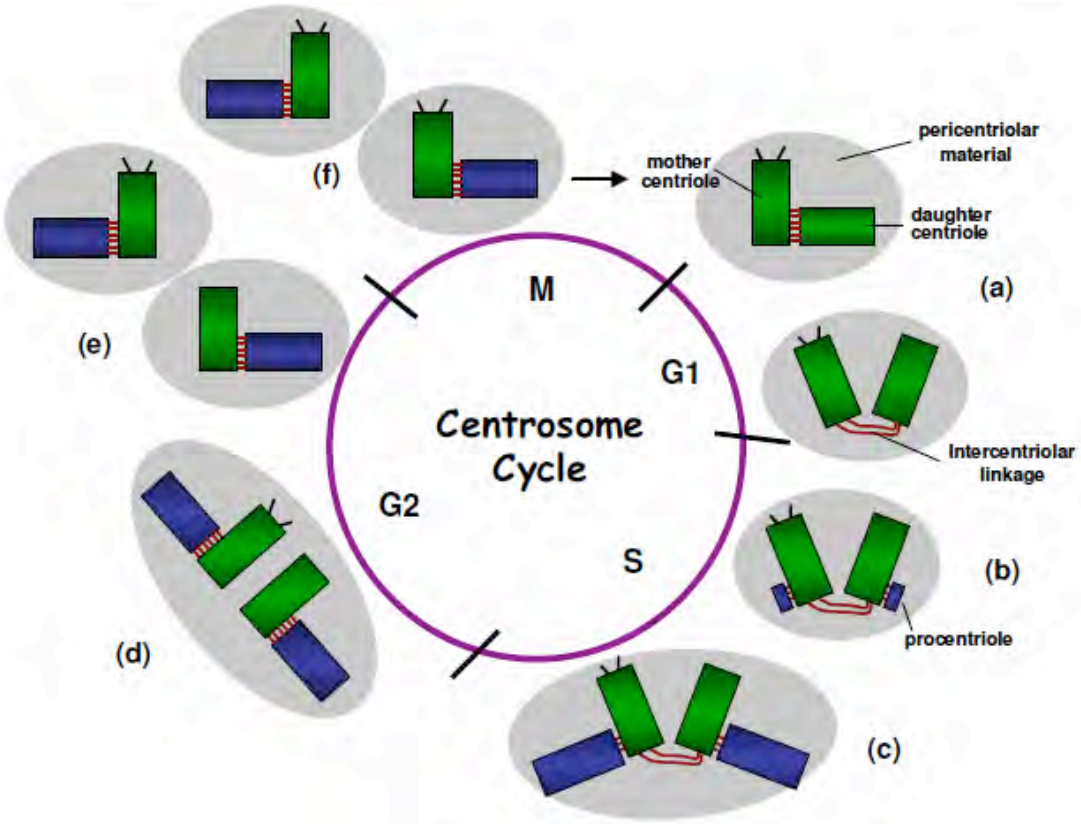

Figure I-2. Centrosome Duplication Cycle. The centrosome must duplicate once and only once during each cell cycle. A.) After mitosis each daughter cell receives one pair of centrioles that have now lost their orthogonal configuration, termed disengagement. B.) As the cell progresses from G1 into S phase a procentriole forms at the proximal end of each mother centriole. C.) The procentrioles continue to elongate as the cells progresses from S to G2 phase where they remain orthogonally oriented until mitosis. D.) During late G2 the mother centrioles become disjoined allowing them to organize the spindles. E.) Before mitosis the PCM is divided between the centrioles. F.) During mitosis a pair of engaged centrioles is present at each spindle pole and the daughter centriole acquires appendages. Mother and daughter centrioles are shown in green, procentrioles are blue and the PCM is in grey. Mother centrioles contain appendages shown as black lines. This figured was reproduced from Crasta and Surana, 2006 (no permission needed).

However, recent evidence demonstrates that a Plk4-mediated cascade leads to the centrosomal recruitment of several proteins including SAS-4,5,6, CPAP, CP110, Cep135, and gamma-tubulin, which are all indispensable for centriole formation (Dammerman et al., 2008; Rodrigues-Martins et al., 2007; Kleylein-Sohn et al., 2007).

Later, as the cell progresses from S into G2, the newly formed daughter centrioles continue growing, until their full length is reached by the following G1. Also during this time, the centrosomes continue maturing, seen by the accumulation of additional PCM and the addition of appendages on the younger mother centriole. In the final phase, the parental centrioles become disjoined, allowing them to migrate and organize the spindle poles during mitosis.

Block to Centrosome Reduplication

When the centrosome duplicates, it is crucial that each mother centriole produces one and only one daughter centriole. If a cell enters mitosis with more than two centrosomes it raises the chances for multipolar spindle formation, which can lead to genomic instability. Under normal conditions centrosomes will duplicate only once, even when the cell contains the subunits sufficient to assemble many centrioles (Sluder at al., 1990; Gard et al., 1990). Further, if untransformed cells are arrested during S-phase, which is permissive for

duplication, centrosomes still maintain proper copy number. However, the question still remains as to how cells precisely control this once and only once duplication.

In 2003, Wong and Stearns provided strong evidence for a centrosome intrinsic block to reduplication. The authors demonstrated that when G1, S, and G2 phase cells were fused together in various combinations, only the unduplicated centrosomes from the G1 cells were able to duplicate when the cells entered S-phase. Thus, something intrinsic to the G2 centrosome was able to block reduplication. Later, it was shown that activation of the protease, Separase, during the metaphase-anaphase transition leads to the disengagement of mother-daughter centrioles and without this disengagement they could not duplicate during the following S-phase (Tsou and Stearns, 2006). This result suggested that the physical association between the mother and daughter centrioles is responsible for preventing the formation of extra centrioles. This hypothesis was further explored by a study where the daughter centriole of the centrosome was laser ablated in S-phase arrested cells. They found that the mother was able to assemble new daughter centrioles within 4 hours of ablation, which furthered the belief that the presence of the daughter centriole prevents the mother from reduplicating (Loncarek et al., 2008).

While the previous studies demonstrate that the presence of the daughter plays a role in blocking reduplication, it does not answer how the mother only forms one centriole at a time during S-phase. In some instances during the laser

ablation studies, the mother produced multiple daughters at one time, suggesting the formation of procentrioles is not limited to one specific spot on the mother centriole (Loncarek et al., 2008). Further, overexpression of Plk4, SAS-6, pericentrin, or CPAP leads to the production of multiple daughter centrioles around the mother centriole (Kleylein-Sohn et al., 2007; Rodrigues-Martins et al., 2007; Loncarek et al., 2008a, Kohlmaier et al., 2009). This data suggests that a tightly regulated equilibrium between multiple kinases and structural proteins must act in concert with structural constraints to regulate centriole duplication (Sluder and Khodjakov 2010).

Centrosome Aberrations and Cancer

Normally, mechanisms exist within cells to properly control centrosome number throughout the cell cycle. However, abnormalities can occur that cause failures in this control, which ultimately lead to centrosome amplification. These abnormalities include centrosome overduplication, centrosome reduplication, and cleavage failure. Centrosome overduplication is characterized by the formation of multiple daughter centrioles around a single mother and can occur due to overexpression of proteins that regulate procentriole formation, the size of the PCM, as well as the length of centrioles. (Kleylein-Sohn et al., 2007; Rodrigues-Martins et al., 2007; Kohlmaier et al., 2009). Centrosome reduplication occurs

when a mother centriole produces multiple daughters one by one, during a single cell cycle. This effect is believed to happen through improper disengagement between the mother and daughter centriole, which will prematurely "license" the mother to duplicate again if conditions are permissive. For example, some cancerous cell lines, such as U2OS cells, can reduplicate their centrioles if S-phase, which is normally permissive for duplication, is experimentally prolonged (Balczon et al., 1995; Stucke et al., 2002). Finally, if defects occur during mitosis and a cell fails cytokinesis, the resulting state is a tetraploid cell containing twice the normal number of centrosomes.

Since centrosomes act in a dominant fashion in the formation of a bipolar spindle, the presence of extra centrosomes during mitosis greatly increases the chance that cells form multipolar spindles **(Figure I-3)**. Such spindles can lead to unequal segregation of chromosomes and ultimately genomic instability due to the gain or loss of alleles. Indeed, centrosome amplification is a common characteristic of both solid and hematological cancers (reviewed in Chan, 2011). In addition, deregulation of genes implicated in cancer, such as p53, also lead to centrosome amplification (Fukasawa et al., 1996; Chiba et al., 2000; Tarapore and Fukasawa, 2002), reviewed in (Fukasawa, 2007; Nigg, 2002).

Interestingly, multipolar mitoses are often detrimental to cells because gross missegregation of chromosomes often leads to death (reviewed in Anderhub et al., 2012). To prevent multipolar mitoses, cells have developed ways to form bipolar spindles in the presence of extra centrosomes.

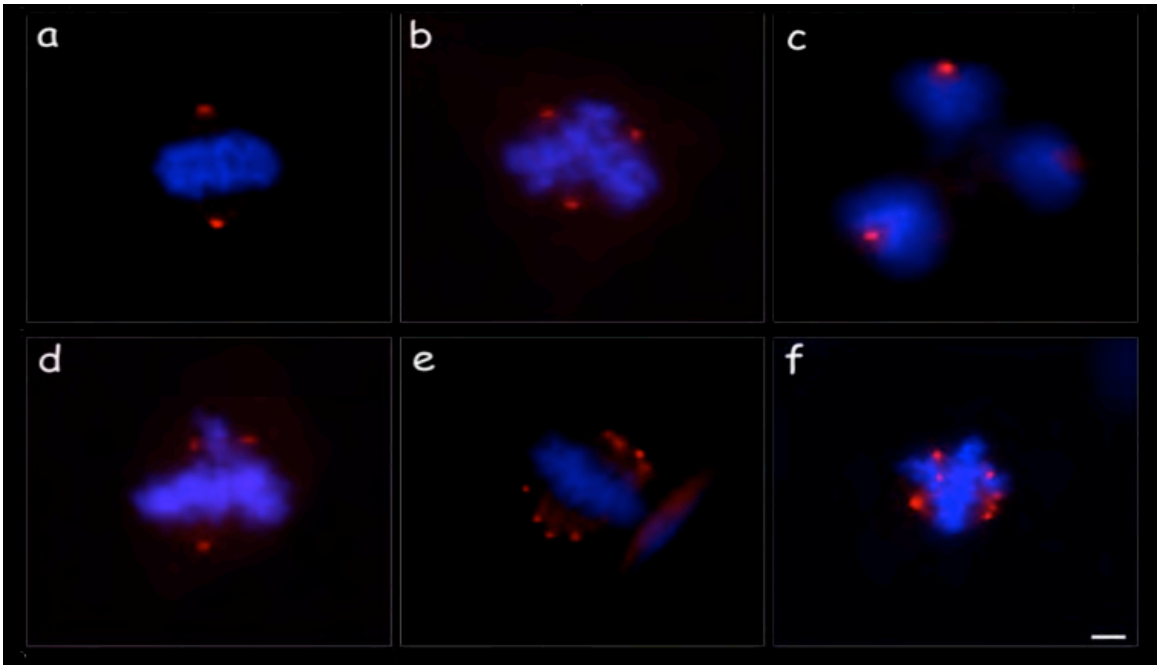

Figure I-3. Spindle Morphologies of p53-/- mouse embryonic fibroblasts. (a) Normal bipolar spindle. (b) Tripolar spindle. (c) Tripolar division. (d) Spindle with two centrosomes at one pole and one centrosome at the other. The spindle with two centrosomes displays one or more chromosome oriented between the centrosomes. (e) Multiple centrosomes clustering to form a bipolar spindle. (f) Many centrosomes forming a multipolar spindle with some bundling at the bottom right. Centrosomes are immunostained for gamma-tubulin (red) and chromosomes are stained blue. This figure is reproduced from Figure 1, Sluder and Nordberg, 2014, with permission from Elsevier.

The most common mechanism is termed centrosome bundling or clustering, where multiple centrosomes coalesce into two spindle poles. Evidence of centrosome clustering is reported in many cancer cells, flies, and even in some non-transformed cell lines (reviewed in Godinho et al., 2009). However, it was shown that before centrosome clustering takes place, cells pass through a multipolar spindle intermediate, which leads to kinetochore-microtubule attachment errors and lagging chromosomes (Ganem et al., 2009). Since many cancer cells cluster extra centrosomes, this provides a strong correlation between centrosome amplification and chromosomal instability and aneuploidy.

DNA Damage and Centrosome Amplification in Transformed Cells

It is widely known that DNA damage leads to centrosome amplification in various transformed cell lines. Reports show that that the incidence of centrosome amplification in transformed cells after ionizing irradiation ranges from 15-65%, depending on the dose and time after irradiation (Sato et al., 2000; Kawamura et al., 2004; Bourke et al., 2007; Shimada et al., 2010). In addition, there are many connections between DNA repair and/or checkpoint proteins and centrosome regulation. For example, expression of a dominant negative mutant of Rad51, a homologous recombination repair protein, or conditional deletion of Rad51 leads to the formation of extra centrosomes (Dodson et al., 2004).

Interestingly, many of these DNA repair and checkpoint proteins also localize directly at centrosomes. For example, ATM and ATR are serine/threonine kinases that are activated early in the DNA damage checkpoint response pathway, but also localize at the centrosome. Additionally, both have been shown to play roles in centrosome regulation (reviewed in Shimada and Komatsu, 2009).

Although many connections between DNA damage, checkpoint proteins, and centrosome regulation are established, exactly how DNA damage leads to centrosome amplification remains mostly a mystery. It is known that a Chk1-dependent prolongation of G2 phase, which involves ATM/ATR, is required for centrosome amplification to occur (Dodson et al., 2004; Bourke et al., 2007; Inanc et al., 2010). However, recent studies provide evidence for several, and perhaps not mutually exclusive, models in transformed cells. The first is that DNA damage leads to the *de novo* formation of extra centrioles. *De novo* formation is the assembly of centrioles without any preexisting centrioles. This event is reported in many cell types including blastomeres (Szollosi et al., 1972), lower eukaryotes (Marshall et al., 2001), and cycling somatic cells when resident centrioles are removed by microsurgery or laser ablation (Khodjakov et al., 2002; La Terra et al., 2005; Uetake et al., 2007). Loffler et al. (2012) report for human lung adenocarcinoma cells that DNA damage leads to the *de novo* formation of centrin-containing centriolar satellites that may serve as platforms for the assembly of extra centrioles that later organize into complete centrosomes

(Loffler et al., 2012).

Another model is that DNA damage leads to the loss of an inhibitory signal that normally blocks centriole reduplication. This idea came from a study where the authors fused irradiated and control populations of G2 phase U2OS cells to test if centrosome amplification occurs through a diffusible stimulatory signal or from the loss of an inhibitory signal. The concept is that an activating signal should be transmissible to the untreated centrosome when the irradiated cells are fused to control cells. They found significantly higher levels of centrosome amplification when the cell fusions contained 2 irradiated cells than 1 irradiated and 1 unirradiated cells, suggesting that an inhibitory signal is lost in the irradiated cells (Inanc, 2010).

A third possibility is that centrosome amplification after DNA damage is the result of cells spending extra time in G2. Interestingly, when both transformed cells and untransformed cells are held in G2 (without DNA damage) using the Cdk1 inhibitor RO-3306 (RO), there was a 50-60% incidence of centrosome amplification (Loncarek et a., 2010). In addition, they found that inhibiting the activity of Plk1 greatly reduced centrosome amplification in RO treated cells. Plk1 is a serine/threonine kinase that plays roles in initiation of mitosis, centrosome maturation, bipolar spindle formation, DNA damage response, and cytokinesis (reviewed in Hyun et al., 2014). Additionally, it has been shown that Plk1 acts early in mitosis to help promote centriole

disengagement (Tsou et a., 2009). Interestingly, Plk1 activity also promotes APC/C activity (Hansen et al., 2004; Moshe et al., 2004), which can independently mediate centriole disengagement and subsequent reduplication of the mother centrioles (Hatano and Sluder, 2012). Furthermore, Prosser et al. (2012) reported that both Plk1 and APC/C activities contribute to centrosome amplification after DNA damage in HeLa cells.

DNA Damage and Centrosomes in Untransformed Cells

Although centrosome amplification after DNA damage is well established in transformed cells, the occurrence in untransformed cells has sparsely been reported and not thoroughly investigated. After ionizing radiation, the incidence of extra centrioles has been reported to only range from 5-10% (Kawamura et al., 2006; Sugihara et al., 2006; Saladino et al., 2009). This is markedly lower than the 15-65% incidence that is reported in transformed cells. However, two of the studies reported centrosome amplification as the incidence of more than two centrosomes as indicated by gamma-tubulin staining. The caveat with this method is that gamma-tubulin localizes in the PCM and appears as a cloud around the centrosome. Therefore, the number of centriole present in each gamma-tubulin cloud cannot be distinguished. For example, if the staining displays three gamma-tubulin foci, it is possible that one contains two centrioles, and the other two contain only one, which would indicate that one pair of

centrioles were disengaged. Indeed, Saladino et al. (2009) reported a 5-15% incidence of centriole disengagement after irradiation of RPE1 cells, as indicated by both centrin and gamma-tubulin staining.

Although the reported incidence of centrosome amplification is less for untransformed cells, even a low level of extra centrosomes poses a threat to the organism if cells repair the DNA damage and continue to proliferate with centrosome amplification. Further, if disengaged centrioles are capable of acting as microtubule organizing centers during mitosis, it raises the incidence of functional centrosome amplification. Therefore, DNA damage to untransformed cells could in principle lead to the generation of an aneuploidy state through altered centriole behavior.

DNA Damaging Agents and Cancer

Cancer victims are often treated with DNA damaging agents, such as ionizing radiation or radiomimetic drugs before or after surgery. Cells respond to DNA damage by activating checkpoint proteins to arrest cells at different points in the cell cycle in order to allow time for repair. This treatment prevents cells from entering S-phase and replicating damaged DNA or entering mitosis and separating damaged DNA into daughter cells. However, if the DNA damage is too severe and cannot be repaired, cell death can occur. Because cancer cells often have relaxed or impaired checkpoint pathways, they are more likely to

replicate damaged DNA increasing the likelihood of cell death (reviewed in Cheung-ong et al., 2013). Although tumor cells are the intended targets, systemic DNA damaging drugs also hit normal proliferating cells in naturally regenerating tissues. This is why patients often suffer from hair loss, nausea and vomiting. Further, post surgical radiation therapy can cause DNA damage in cells of healing surgical wounds. If the DNA damage leads to centrosomal defects, this could lead to genomic instability and normal cells could begin to evolve transformed characteristics. Indeed, formation of secondary tumors after DNA damaging therapies is a recognized problem for cancer victims. For example, the genesis of therapy-related acute myeloid leukemia after treatment for non-Hodgkin lymphoma is a reported problem (Krishnan and Morgan 2007).

Phototoxicity During Live-Cell Imaging

In addition to chemotherapeutic drugs and ionizing radiation, cellular damage can be acquired from various external conditions. For example, ultraviolet light can lead to photo-oxidative damage, especially to skin cells exposed to the sun. Further, blue light can produce photochemical lesions in the retina pigment epithelium (Ham et al., 1980). With the development of fluorescent proteins, these wavelengths of light are now utilized by microscopy techniques to visualize cell structure, function, and physiology in living cells.

These techniques range from long-term time-lapse observations, to advanced methods including fluorescence recovery after photo-bleaching (FRAP), fluorescence resonance energy transfer (FRET), fluorescence lifetime imaging (FLIM**),** ratiometric ion measurements, and multi-photon microscopy (reviewed in Stephen and Allen, 2003; O'Connor and Silver, 2013; Cardullo, 2013; Chen et al., 2013). Additionally, super-resolution techniques such as stimulated emission depletion (STED), structured illumination microscopy (SIM), and photoactivation localization microscopy (PALM) have allowed researchers to begin studying biological structures below the diffraction limit in living cells (reviewed in Godin, 2014). The excitation wavelengths used for these techniques range from the near UV (340-360 nm) for cell permeable Ca++ indicating dyes to the far red (590-630nm) with some of the new generation of red fluorescent proteins and for multi-photon microscopy.

Although live-cell fluorescence microscopy is a powerful tool, a fundamental limitation is the phototoxicity of the high intensity shorter wavelengths needed to image the commonly used fluorescent constructs such as EGFP (reviewed in Magidson and Khodjakov, 2013; Jennifer Waters, 2013). Phototoxicity refers to the negative reaction of tissues and cells to exogenous light energy, often resulting in cellular damage. Photodamage is believed to arise through the light induced formation of chemically reactive free radicals and the formation of singlet and triplet forms of oxygen (Zdolesk et al., 1993; Dixit and Cyr, 2003). This is thought to occur primarily due to excitation of fluorescent

molecules into more reactive states, where they can interact with the molecular environment.

Acquiring Photodamage

Although photodamage may not be an issue for short-term observations where only a few images are captured, it is a serious problem for applications involving long-term observations. This is especially true when each time point requires taking a Z stack and/or if more than one fluorescent protein is being visualized. Further, advanced applications such as FRAP and FRET, and many super-resolution techniques use high power lasers and the illumination intensities required can severely damage living cells. In addition to the techniques themselves, imaging equipment can also contribute to unnecessary exposures. For example, imprecise hardware synchronization between the shutter and camera can lead to actual exposure times becoming longer than what is intended (see Magidson and Khodjakov, 2013). This example again becomes a greater problem when multiple Z-stacks are being acquired and if more than one color is being visualized. Importantly, photodamage can begin even before the imaging sequence begins. For example, time spent scanning the slide, identifying cells of interest, and bringing them into to focus can require a minimum of several seconds, the equivalent of many imaging exposures.

Consequences of Photodamage

The most obvious consequence of photodamage is cell death as seen by membrane blebbing, cell rounding, and apoptosis (Zdolesk et al., 1990; Dixit and Cyr 2003; Hoebe et al., 2007; Kuse et al., 2014). However, cell death is paradoxically the best outcome of photodamage because the cellular changes are visually obvious and researchers will immediately know the experimental results have been impacted. A more pernicious problem is that photodamage is manifested as subtle changes to cellular physiology and viability. For example, illumination of mid-prophase PtK cells with 488nm light leads to chromosome decondensation and the return of cells to a G2-like state (Khodjakov and Reider, 1999). Further, fluorescently labeled microtubules can break both *in vivo* and *in vitro* upon exposures to high intensities of blue or green light (Vigers et al., 1988; Guo et al., 2006). These changes may lead to observations that are deemed important, whereas they could simply be artifacts from photodamage. Moreover, well before the cell visibly dies, the cell can sustain substantial functional damage, which may not be evident until later if the observations last long enough (see Magidson and Khodjakov, 2013).

Some examples of functional photodamage, short of cell death, include studies of the proliferative capacity of yeast and embryonic *C. elegans* cells (Carlton et al., 2010; Tinevez et al., 2012). Carlton et al. (2010) measured yeast cell doublings 20 hours after exposure to varying intensities of blue light. They

found that high intensities of blue light arrested or killed cells and little to no cell division had occurred. They determined that the light intensity needed to be reduced two fold to observe unperturbed viability. Tinevez et al. (2012) exposed *C. elegans* embryos to repeated cycles of blue light exposures for 2 hours and then characterized the total number of cells formed compared to control embryos. Using increasing intensities of blue light they found that low intensity light had no effects, but above a certain threshold ($4.27X10^{-2}$ J/cm^2/stack) there was a sharp decline in the total number of cells formed.

Experimental Stress and Photodamage

In addition to the direct consequences, photodamage also acts as a cellular stress making cells susceptible to experimental treatments. Since stress is additive, stresses that are singly of little consequence can act additively to significantly impact cell physiology and behavior. For example, multiple studies provided evidence that the removal of the centrosome from mammalian cells causes a G1 cell cycle arrest (Hinchcliffe et al. 2001; Khodjakov and Rieder, 2001). However, a later investigation demonstrated that this arrest resulted from the combined stresses of centrosome removal, culture conditions, and microsurgery or blue light exposures during laser ablations of GFP centrin tagged centrioles (Uetake et al., 2007). Similarly, experimental treatments such as drug

treatments and RNAi can also sensitize cells to additional stressors. For example, the percentage of Ptk cells that undergo cell cycle reversion after blue light exposures (see above) is greater if the cells are first treated with antimicrotubule drugs (Khodjakov & Rieder, 1999).

Current Understanding of Phototoxicity

Traditionally the most commonly used excitation wavelengths are blue (488nm) for EGFP and green (~546nm) for the RFPs. Although the damaging effects of blue light are well recognized (reviewed in Waters, 2013), most studies have focused their assays on cell death. Cells that experience photodamage, but remain alive could exhibit phenotypes to the researcher that are merely artifacts, greatly complicating experimental analysis. Therefore, a more sensitive assay of characterizing phototoxic effects of light is needed. Further, the extent to which green light damages mammalian somatic cells has not been systematically tested. Green light has been generally assumed to be benign, but, should this not be the case, investigators will have to evaluate whether the use of RFP constructs is worthwhile given their lower brightness relative to EGFP and the consequent need for longer excitations per image.

Summary

The work presented in this thesis comprises two separate studies investigating the effects of cellular damage.

Chapter II focuses on the characterization of centriole behavior after DNA damage in untransformed human cells. While centrosome amplification after DNA damage in transformed cells is widely known, the effects in untransformed cells have not been well characterized. We were particularly interested in answering several questions. First, we wanted to understand why the reported incidence of centrosome amplification was much higher in transformed cells compared to untransformed cells. We also examined why DNA damage leads to a high incidence of centriole disengagement without reduplication in our cells. Further, we explored the roles of Plk1 and APC/C in DNA damage induced centriole disengagement. Finally, we determined if cells that escaped from the G2 cell cycle arrest and entered mitosis, did so with disengaged or extra centrioles and what the outcome of such mitoses were.

The work in **Chapter III** provides a practical assessment of photodamage during live-cell imaging. This study had two main objectives. The first goal was to systematically characterize the phototoxicity of blue (488nm) and green (546nm) light on the cell cycle progression of untransformed human cells (RPE1) with and without the expression of fluorescent proteins. These wavelengths are commonly used during fluorescence microscopy and while blue light is known to

be harmful, the effects of green light on mammalian somatic cells have not been characterized.

The second objective was to test three different strategies that could be used to reduce the phototoxic effects of blue light. First, we tested if using lower intensity light for longer times allows cells to buffer the effects of photodamage better than when short, high intensity exposures are used. Second, we wanted to know if adding a long-pass filter to block possible leakage of short wavelength light, known to be extremely damaging to cells, could mitigate the phototoxicity. Finally, we tested if reducing the production of reactive oxygen species through low oxygen growth conditions or the addition of a free radical scavenger could improve tolerance for blue light.

PREFACE TO CHAPTER II:

This work presented in this chapter appears in:

Douthwright and Sluder. Link Between DNA Damage and Centriole Disengagement/Reduplication in Untransformed Human Cells. J Cell Physiol (2014) 229:1427-1436.

CHAPTER II: Link Between DNA Damage and Centriole Disengagement/Reduplication in Untransformed Human Cells

Abstract

The radiation and radiomimetic drugs used to treat human tumors damage DNA in both cancer cells and normal proliferating cells. Centrosome amplification after DNA damage is well established for transformed cell types but is sparsely reported and not fully understood in untransformed cells. We characterize centriole behavior after DNA damage in synchronized untransformed human cells. One hour treatment of S phase cells with the radiomimetic drug, Doxorubicin, prolongs G2 by at least 72 hours, though 14% of the cells eventually go through mitosis in that time. By 72 hours after DNA damage we observe a 52% incidence of centriole disengagement plus a 10% incidence of extra centrioles. We find that either APC/C or Plk activities can disengage centrioles after DNA damage, though they normally work in concert. All disengaged centrioles are associated with γ-tubulin and maturation markers and thus, should in principle be capable of reduplicating and organizing spindle poles. The low incidence of reduplication of disengaged centrioles during G2 is due to the p53 dependent expression of p21 and the consequent loss of Cdk2 activity. We find that 26% of the cells going through mitosis after DNA damage contain disengaged or extra centrioles. This could produce genomic instability through transient or persistent spindle multipolarity. Thus, for cancer patients the

use of DNA damaging therapies raises the chances of genomic instability and evolution of transformed characteristics in proliferating normal cell populations.

Introduction

The centrosome is the primary microtubule-organizing center (MTOC) of the interphase mammalian cell. In preparation for mitosis the centrosome duplicates, and the sister centrosomes later determine the essential bipolarity of the spindle. Since centriole pairs collect the pericentriolar material (PCM) that forms the MTOC, the duplication of the centrosome as a whole is determined by the duplication and separation of centriole pairs (Sluder and Rieder, 1985).

Centriole duplication starts with the functional separation, or disengagement, of mother from daughter centrioles during anaphase; this event is necessary to "license" both centrioles for duplication in the following S phase (reviewed in Nigg and Stearns, 2011). Centriole disengagement is mediated by APC/C activity that leads to the degradation of securin thereby releasing the proteolytic activity of separase (Zou et al., 1999; Tsou and Stearns, 2006). Separase activity opens the centromeric cohesin complexes and cleaves the PCM scaffolding elements kendrin/pericentrin B (Matsuo et al., 2012; Lee and Rhee, 2012). Additionally Plk1 activity in early mitosis also contributes to separase dependent and independent centriole disengagement. Although APC/C and Plk1 activities can individually cause centriole disengagement, they

normally work in concert to ensure the timeliness and fidelity of disengagement in anaphase (Tsou et al. 2009; Hatano and Sluder, 2012).

Centriole overduplication or reduplication leads to the formation of extra centrosomes (centrosome amplification) that increases the chances that the cell will assemble a multipolar spindle at mitosis, which can lead to whole chromosome gains and losses (reviewed in Brinkley, 2001; Cimini et al., 2001; Nigg, 2002; Ganem et al. 2009). Also, spindle multipolarity, even transient multipolarity, leads to lagging chromosomes in anaphase. Such laggards often become micronuclei that show delayed or incomplete DNA synthesis and consequently such chromosomes become grossly damaged when the cell enters mitosis (Ganem et al., 2009, Crasta et al., 2012). The resulting genomic instability can lead to loss of normal alleles for tumor suppressor genes and other genetic imbalances that promote unregulated growth characteristics and diminished apoptotic response to cellular damage (reviewed in Orr-Weaver and Weinberg, 1998; Nigg, 2002). Indeed, pre-invasive carcinomas and most late-stage human solid tumor cells show a high incidence of centrosome amplification that is thought to contribute to multi-step carcinogenesis (Lingle and Salisbury, 2000; Pihan et al., 2001; Pihan et al. 2003; Lengauer et al., 1998; Lingle et al. 2002; Kramer et al., 2002; D'Assoro et al., 2002; Goepfert et al., 2002; Weaver et al., 2007; Basto et al., 2008).

Cancer victims are often treated with DNA damaging agents, such as ionizing radiation or radiomimetic drugs before or after surgery. Although tumor

cells are the intended targets, systemic DNA damaging drugs also hit normal proliferating cells in naturally regenerating tissues. Post surgical radiation therapy can cause DNA damage in cells of healing surgical wounds. If the DNA damage leads to defects that influence genomic stability, these proliferating cells could begin to evolve transformed characteristics. Indeed, formation of secondary tumors after DNA damaging therapies is a recognized problem for cancer victims. For example, the genesis of therapy-related acute myeloid leukemia after treatment for non-Hodgkin lymphoma is a reported problem (reviewed in Krishnan and Morgan 2007).

Centrosome amplification after DNA damage is a well-established phenomenon that has been studied almost entirely in various transformed cell types. It is associated with a Chk1 dependent prolongation of G2 phase (Dodson et al., 2004; Bourke et al., 2007; Inanc et al., 2010). The incidence of centrosome amplification reported for irradiated transformed cells ranges from 15-65%, depending on the dose and time after irradiation (Sato et al., 2000; Kawamura et al., 2004; Bourke et al., 2007; Shimada et al., 2010). Although the basis for centrosome amplification after DNA damage has been uncertain, recent studies provide evidence for several, and perhaps not mutually exclusive, pathways in transformed cells. Loffler et al (2012) report for human lung adenocarcinoma cells that DNA damage leads to the *de novo* formation of centrin containing centriolar satellites that may serve as platforms for the assembly of extra centrioles that later organize complete centrosomes. Inanc et

al. (2010) report that DNA damage leads to the loss of an inhibitory signal that normally blocks centriole reduplication. Another possibility is that centrosome amplification after DNA damage is the consequence of the cells spending extra time in G2. When cells (without DNA damage) are held in G2 with the Cdk1 inhibitor RO-3306, rising Plk1 activity leads to repeated centriole disengagement and reduplication resulting in a 50-60% incidence of centrosome amplification (Loncarek et al., 2010, Prosser et al., 2012). Plk1 activity also promotes APC/C activity (Hansen et al., 2004; Moshe et al., 2004), which can separately mediate centriole disengagement and subsequent reduplication of the mother centrioles (Hatano and Sluder, 2012). Prosser et al. (2012) report that both Plk1 and APC/C activities participate in causing centrosome amplification after DNA damage in HeLa cells.

Although DNA damage induced centrosome amplification is well established for transformed cells, its occurrence in untransformed cells has been sparsely reported and not thoroughly investigated. After DNA damage, the incidence of extra centrioles has been reported to range from 5-10% and there can be a 5-15% incidence of disengaged but not duplicated centrioles (Kawamura et al., 2006; Sugihara et al., 2006; Saladino et al., 2009). Even this level of centrosome amplification could pose a threat to the organism if some cells repair the DNA damage and continue to proliferate.

We systematically characterized centriole behavior after DNA damage in synchronized untransformed human cells. We were particularly interested in

several issues. We wanted to test the roles of Plk and APC/C activities separate from each other in centriole disengagement after DNA damage. We also asked why the reported incidence of extra centrosomes for untransformed cells after DNA damage is lower than that found in transformed cells. If centrosome amplification after DNA damage is simply the consequence of the cells spending extra time in G2, we wanted to know why the incidence of centrosome amplification after DNA damage is significantly lower than that in cells without damaged DNA that are arrested in G2 with a Cdk1 inhibitor. We also examined why centriole disengagement after DNA damage does not lead to much reduplication. Lastly, continuous time-lapse observations also allowed us to precisely determine the behavior of the low percentage of untransformed cells that escaped G2 arrest and divided - some with extra centrosomes.

Results

DNA damage prolongs G2

We used untransformed human cells (RPE1) stably expressing GFP-centrin 1 to tag individual centrioles. These cells have an intact p53 pathway; centriole duplication and mitosis are normal.

We first characterized the extent to which DNA damage prolongs G2. To avoid the ambiguities of interpreting the various behaviors of cells from asynchronous populations, we shook off mitotic cells to provide synchronized

populations. Twelve hours later, a time when 85% of cells were EdU positive (had at least entered S phase), we treated them with the radiomimetic drug Doxorubicin for 1 hour to induce DNA damage **(Figure II-1A)**. Four hours after drug washout all cells had γH2AX foci in the nuclei confirming DNA damage **(Figure II-1A, images)**. Whereas, 90% showed numerous γH2AX foci, the remainder had at least several foci. We continuously followed 97 Doxorubicin treated cells for 3 days by time-lapse video microscopy and found that 100% remained in interphase through the first 24 hours. At 48 hours 90% were still in interphase and by 72 hours 86% had failed to enter mitosis. The remaining 14% all divided and cleaved in a bipolar fashion. Seventy six percent of the resulting daughter cells arrested in interphase and never progressed onto mitosis. The other 24% divided once again in a bipolar fashion before the filming runs were terminated. Thus, DNA damage led to a substantial and variable prolongation of G2 in all cells but did not permanently arrest 14% of them.

Centriole disengagement and maturation during prolonged G2

We fixed synchronized cell populations at 24, 48, and 72 hours after Doxorubicin washout and immunostained for C-Nap1, a protein that participates in linking sister centrosomes together **(Figure II-1A protocol diagram)**. Centriole disengagement was determined by the spacing of GFP-centrin foci as well as the ratio of centrin to C-Nap1 spots (Tsou and Stearns, 2006). When mother-daughter centrioles are engaged, two closely paired centrin spots are

associated with a single C-Nap1 spot (2:1 Centrin:C-Nap1). When centrioles disengage, the centrin spots are further apart and there is a C-Nap1 spot associated with each centrin spot (1:1 Centrin:C-Nap1).

Control G2 cells at 17hrs after mitotic shake-off exhibited 1% incidence of disengaged centrioles. For cells in G2 after DNA damage the incidence of disengaged centrioles increased to 22% at 24 hours and to 52% at 72 hours **(Figure II-1B)** as seen by separation of individual centrin foci each associated with a C-Nap1 spot (3 experiments – 200 cells scored per experiment) **(Figure II-1C)**. Many cells showed four separated centrin foci and others contained two separate centrin foci and two closely paired foci indicating that centrioles in only one G2 centrosome had disengaged. The range of distances between GFP-centrin foci rose from 0.26-0.65um in control G2 cells to 0.33-33um in cells 24 hours after Doxorubicin washout **(Figure II-1D)**.

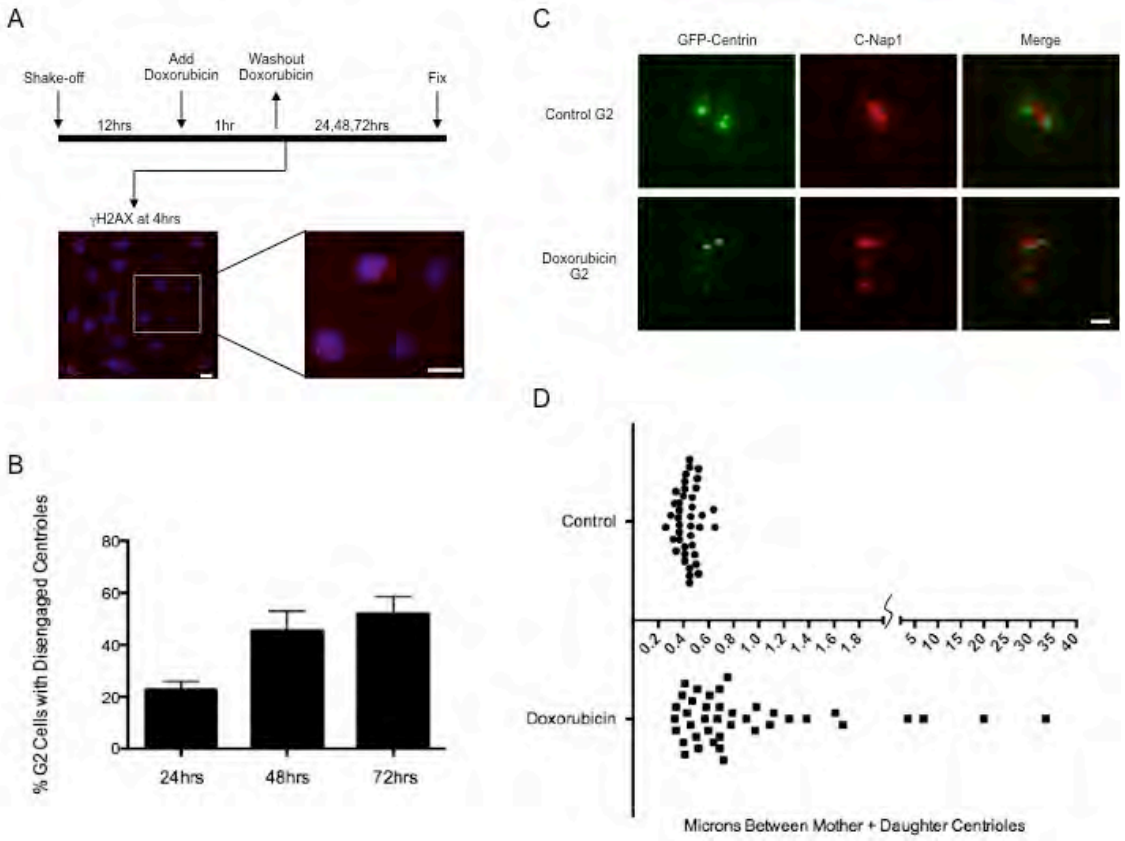

Figure II-1. Doxorubicin induced DNA damage leads to centriole disengagement during prolonged G2 phase. (A) Diagram of experimental protocol. Left image shows a 10X field of cells stained for γH2AX (red) and DNA by Hoechst (blue) 4 hours after the 1 hour Doxorubicin pulse. Right image is an enlargement of a portion of left image showing range of γH2AX labeling. Scale bars= 40μm. (B) Incidence of G2 cells with disengaged centrioles at 24, 48, and 72hrs after DNA damage. Disengagement determined by a 1:1 ratio of Centrin:C-Nap1 spots. Histogram bars indicate the average from at least 3 experiments with 200 cells counted for each condition. Error bars are one standard deviation. (C) Representative images of centrioles in control G2 cells and cells with disengaged centrioles 48hrs after Doxorubicin treatment. GFP-centrin1 (green), C-Nap1 (red). Scale bar=1μm. Images are maximum intensity point projections from Z series images. (D) Graph representing the distances between mother and daughter centrioles in control G2 cells and cells 24hrs after Doxorubicin treatment. Each dot represents the distance between one pair of mother-daughter centrioles. Microns between centrioles are shown along the X axis. Forty centriole pairs were measured for each condition.

Wang et al (2011) reported that daughter centrioles go through Plk1 dependent “modification” indicative of maturation during mitosis, which is required for them to duplicate and organize a MTOC during the following cell cycle. These modifications include the loss of SAS-6 as well as the recruitment of C-Nap1 and γ-tubulin. We wanted to determine if the disengaged centrioles in our experiments, particularly the daughters, matured during the prolonged G2 and thus, could in principle duplicate thereby amplifying centriole number. We fixed cell populations 48 hours after Doxorubicin washout and immunostained separately for SAS-6, a cartwheel protein found in daughter centrioles; CEP170, an appendage protein found on mother centrioles; and γ-tubulin. These cells were compared to control G2 cells (14 hours after shake-off) containing two pairs of engaged centrioles. We observed that 92% of control G2 cells have 2 SAS-6 spots (one at each daughter centriole), while 94% of Doxorubicin treated cells with disengaged centrioles showed no SAS-6 staining at disengaged centrioles **(Figure II-2, top)**. Ninety-eight percent of the control cells contained two CEP170 spots, while 91% of Doxorubicin treated cells with disengaged centrioles showed 4 CEP170 spots **(Figure II-2, middle)**. Lastly, 98% of Doxorubicin treated cells contained 4 γ-tubulin clouds associated with the separate centrin spots, while 96% of control cells showed only 2 γ-tubulin clouds **(Figure II-2, bottom)**. Together these observations indicate that disengaged daughter centrioles are “modified” during prolonged G2 and should, in principle, be capable of duplicating again.

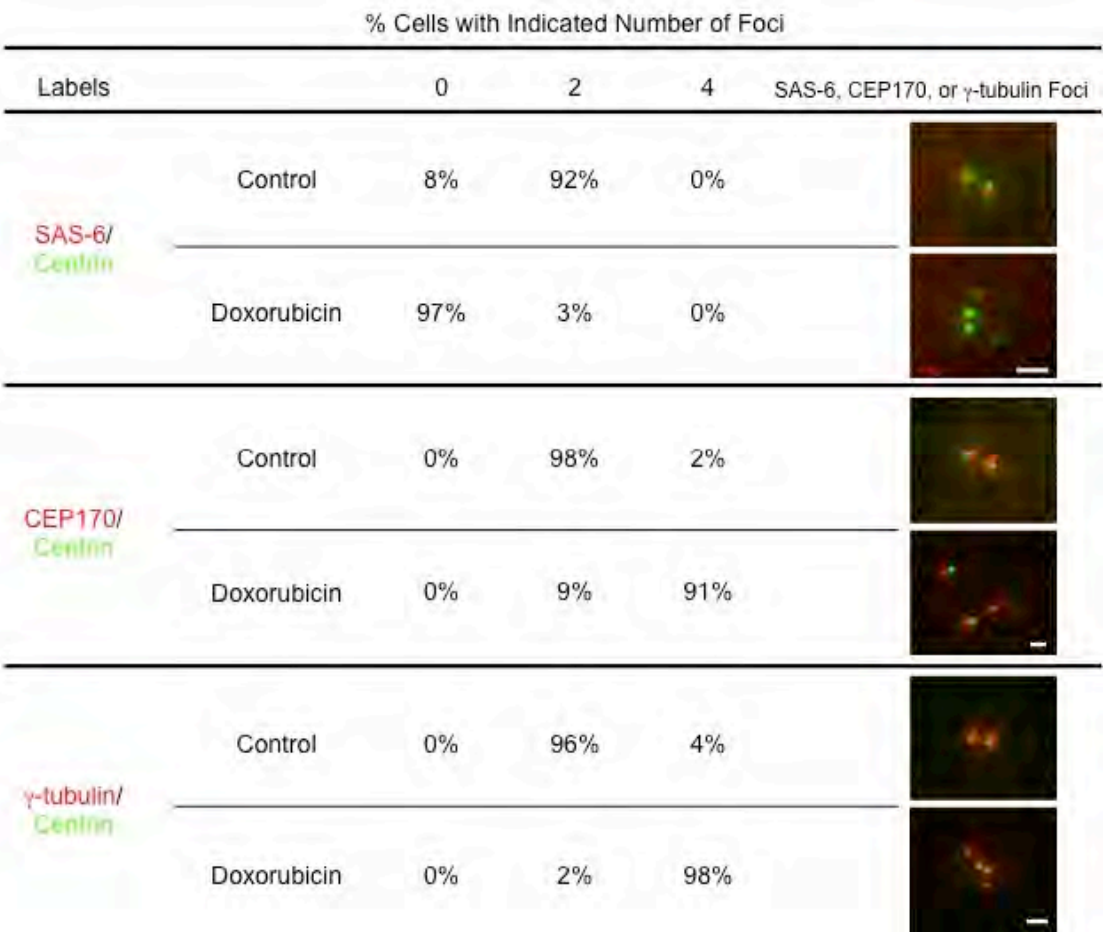

Figure II-2. Disengaged centrioles display markers of maturation after DNA damage. Numbers shown represent percentage of cells that contain 0, 2, or 4 foci of SAS-6 (top), CEP170 (middle), or γ-tubulin (bottom) associated with centrin foci for control G2 cells and cells 48 hours after Doxorubicin treatment. Percentages are based on 150 cells observed per condition. Images of centrioles in control cells and disengaged centrioles in Doxorubicin treated cells show GFP-centrin in green and SAS-6, CEP170, or γ-tubulin in red. Chosen images represent most prevalent phenotype for each condition. Scale bars=1μm. Images are maximum intensity point projections from Z series images.

Plk and APC/C activities in centriole disengagement after DNA damage

Precisely how centrioles disengage after DNA damage has been unclear. When transformed and untransformed cells (no DNA damage) are arrested in G2 with the Cdk1 inhibitor RO-3306 (hereafter RO), Plk1 and APC/C activities mediate centriole disengagement, which allows centriole reduplication (Loncarek et al., 2010; Prosser et al., 2012; Hatano and Sluder 2012). Therefore, we tested whether Plk and APC/C activities, alone or in combination, promoted centriole disengagement after DNA damage.

We synchronized cells in S with thymidine for 17 hours, released them, and 3 hours later pulsed with Doxorubicin for 1 hour. Immediately after the Doxorubicin pulse we added the Plk inhibitor (BI 2536), an APC/C inhibitor (proTAME), or both **(Figure II-3A)**. BI 2536 at the 200nM concentration we used should completely inhibit Plk1 activity and largely block Plk2 and Plk3 activities (Steegmaier et al., 2007). To empirically test the efficacy of proTAME in inhibiting APC/C activity we treated thymidine synchronized control cultures (no DNA damage) with 12uM proTAME after thymidine release and followed 50 cells by time-lapse video microscopy. 80% of the cells arrested in prometaphase for 12 hours, 60% remained in prometaphase for 24 hours, and 48% arrested in prometaphase for at least 30 hours.

Inhibition of Plk activity alone slightly diminished the incidence of centriole disengagement 24 hours after Doxorubicin treatment **(Figure II-3B)**. In contrast, inhibition of APC/C activity alone resulted in a decrease in centriole

disengagement at this time **(Figure II-3B)**. 48 hours after Doxorubicin treatment, the incidences of centriole disengagement after Plk or APC/C inhibition singly were similar to those found after Doxorubicin treatment only **(Figure II-3B,C)**. However, when Plk and APC/C activity were both inhibited, there was a marked decrease in the incidence of centriole disengagement at 24 and 48 hours after Doxorubicin treatment **(Figure II-3B,C)**. These observations indicate that APC/C activity is the primary driver of centriole disengagement in the first 24 hours and by 48 hours either Plk or APC/C activity singly can drive centriole disengagement. Thus, Plk1 and APC/C activity play independent, but redundant roles in centriole disengagement after DNA damage in RPE1 cells (see also, Hatano and Sluder, 2012).

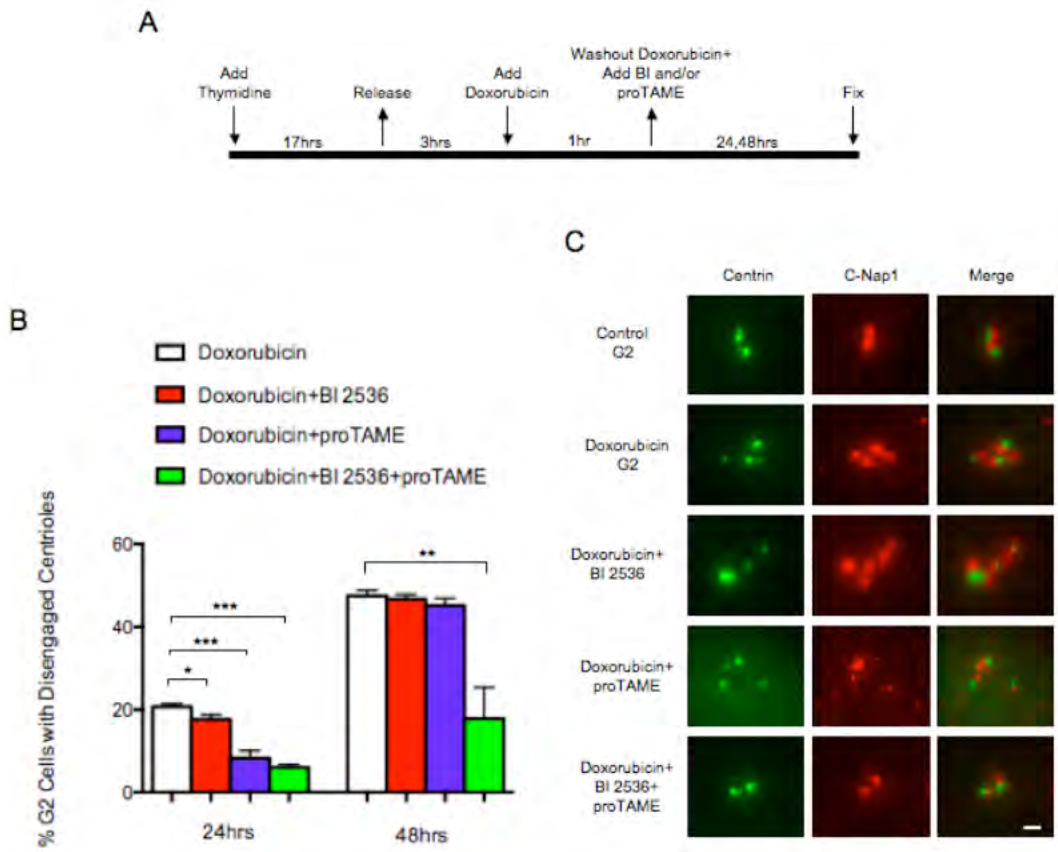

Figure II-3. Centriole disengagement after DNA damage is due to the independent activities of Plk and APC/C. (A) Diagram of experimental protocol. (B) Incidence of G2 cells with disengaged centrioles at 24 and 48 hours after addition of Doxorubicin with indicated treatments. Disengagement determined by a 1:1 ratio of Centrin:C-Nap1 spots. Histogram bars indicate the average from at least 3 experiments with 200 cells counted for each condition. Error bars are one standard deviation. *$p \leq 0.05$, **$p \leq 0.01$, ***$p \leq 0.001$, determined by a two-tailed unpaired Student's t test. (C) Representative images of centrioles in a control G2 cell and in cells 48 hours after Doxorubicin treatment or 48hours after treatment with Doxorubicin plus either 200nM BI 2536, 12μM proTAME, or both. GFP-Centrin (green), C-Nap1 (red). Scale bar=1μm. Images are maximum intensity point projections from Z series images.

Centriole reduplication during prolonged G2

We characterized the extent to which disengaged centrioles reduplicate after DNA damage. Since we found that all disengaged centrioles were associated with the maturation markers, they should in principle be capable of duplicating during G2. We fixed cells at 24, 48, and 72 hours after Doxorubicin treatment and counted cells exhibiting more than 4 centrin foci (3 experiments – 200 cells scored per time point). Control G2 populations (no DNA damage) exhibited a 0.5% incidence of extra GFP-centrin foci. 24 hours after Doxorubicin treatment 3.5% of the cells contained 5-8 GFP-centrin foci. At 48 hours, 4.8% contained extra centrin foci and by 72 hours after treatment the incidence of extra foci rose to 10% **(Figure II-4A,B)**. For all cells, every centrin focus was associated with γ-tubulin indicating that they were centrioles not centrin containing pericentriolar satellites (Loffler et al., 2012) **(Figure II-4A,C)**.

We previously noted that by 72 hours after DNA damage 14% of the cells eventually overcame the G2 arrest and went through mitosis. Cleavage failure has been reported for cells dividing after DNA damage (Varmark et al., 2009). Two sorts of observations indicate that simple cleavage failure is not the source of extra centrioles in our DNA damaged cells. First, induction of cleavage failure in RPE1 cells invariably leads to binucleate cells in the first post cleavage failure cell cycle (Krzywicka-Raka and Sluder, 2011); none of the cells containing extra centrioles after DNA damage were binucleate. Second, we circled fields of cells after Doxorubicin treatment and continuously followed them for 72 hours before

fixing and immunostaining for γ-tubulin and C-Nap1. We relocated 100 cells that remained in interphase for the entire duration of the films and found 10% contained extra centrin foci, all colocalizing with γ-tubulin or C-Nap1 **(Figure II-4C)**. This confirms that extra centrioles assembled during prolonged G2 after DNA damage.

Limits on the reduplication of disengaged centrioles

The 10% incidence of centriole reduplication we observe after DNA damage is substantially less than the 60% incidence found when RPE1 cells without DNA damage are held in G2 by inhibition of Cdk1 activity (Loncarek et al., 2010) and less than the 15-65% incidence of centrosome amplification after DNA damage in transformed cell lines (Sato et al., 2000; Kawamura et al., 2004; Bourke et al., 2007; Shimada et al., 2010). These differences prompted us to investigate what limits the reduplication of disengaged centrioles that should in principle be capable of doing so.

DNA damage in untransformed cells leads to p53 accumulation and the consequent expression of the Cdk inhibitor p21 (reviewed in Zhou and Elledge, 2000). Cdk2 activity initiates centriole duplication (reviewed in Hinchcliffe and Sluder 2002) and is needed for centrosome amplification after DNA damage (Hanashiro et al., 2008; Bourke et al., 2010). To test if p53 activity after DNA damage suppressed duplication of disengaged centrioles, we knocked down p53 in Doxorubicin treated cells and assayed for changes in the incidence of centriole

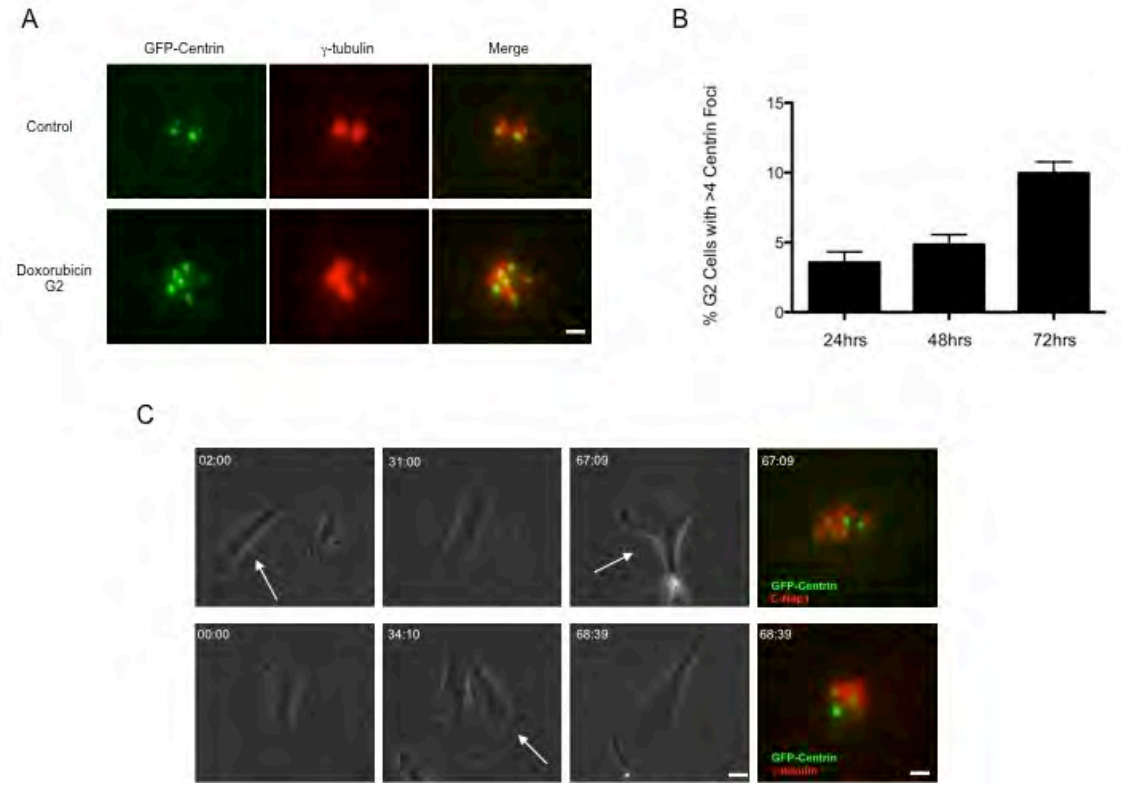

Figure II-4. DNA damage leads to low levels of centriole reduplication during prolonged G2. (A) Representative images of centrioles in a control G2 cell and extra centrioles in a cell 48hrs after Doxorubicin. GFP-centrin (green), γ-tubulin (red). Scale bar=1μm. Images are maximum intensity point projections from Z series images. (B) Incidence of cells with more than four centrin foci colocalizing with γ-tubulin at 24, 48, and 72hrs after addition of Doxorubicin. Histogram bars indicate the average from at least 3 experiments with 200 cells counted for each condition. Error bars are one standard deviation. (C) Correlative phase contrast/immunofluorescence images of G2 arrested cells exhibiting more than four centrin foci colocalizing with γ-tubulin (upper panels) or C-Nap1 (lower panels). Phase contrast images were taken at 10X magnification and corresponding immunofluorescence images were acquired at 100X magnification. Arrows depict cell that was followed. GFP-centrin (green), γ-tubulin (red), C-Nap1 (red). Scale bars= 20μm and 1μm respectively. hr:min shown in upper left corner of each frame represents time after Doxorubicin pulse. Fluorescence images are maximum intensity point projections from Z series images.

reduplication. This allowed us to cleanly assess the role of p53 in untransformed cells without the suite of defects found in cancer-derived cells. This also served as a model for normal cells that may suffer loss of heterozygosity for tumor suppressing genes during chemotherapy with DNA damaging agents.

We transfected asynchronous cultures with siRNA for p53 and 12 hours later shook-off mitotic cells. Twelve hours later these cells were treated with Doxorubicin for 1 hour and then continuously followed by time-lapse video microscopy. For 48 hours after the Doxorubicin treatment 54% remained in interphase while the rest of the cells entered mitosis between 24 and 48 hours. The duration of mitosis (cell rounding to the onset of daughter cell flattening) averaged 45 minutes in control cells and was prolonged 2 – 12 hours in 55% of the treated cells. Of the cells that underwent prolonged mitosis, 5% failed cleavage and 18% divided in a multipolar (15% tripolar; 3% tetrapolar) fashion.

To assay for centriole amplification in p53 knock down cells after DNA damage we followed marked fields of cells for 34 hours after Doxorubicin treatment (a time when 87% of cells were still in interphase). At this time preparations were fixed and immunostained for γ-tubulin to complement the GFP centrin signals. We relocated the fields of cells previously followed *in vivo* and counted centriole number in 152 cells we knew had remained in interphase. We found that 27% of such cells contained 5 to 8 centrin foci, all colocalizing with γ-tubulin, compared to 3% at this time for Doxorubicin treated cells with an intact p53 response **(Figure II-5A,B)**.

We tested for p21 expression after DNA damage for cells treated with Doxorubicin only (no siRNA for p53). We found that by 12 hours after the Doxorubicin pulse 95.5% of cells exhibited expression and nuclear localization of p21, compared to only 10% of G2 control cells 15 hours after mitotic shake off. Seventy-two hours after Doxorubicin treatment, 93.5% of the cells still exhibited nuclear p21 staining, a time when 52% of cells exhibit disengaged centrioles **(Figure II-5C, upper row of images)**. We did not observe increased expression and nuclear localization of p27 as was reported for neuroblastoma cells after ionizing radiation (Sugihara et al., 2006) **(Figure II-5C, lower row of images)**. We also observed that p21 expression levels after DNA damage were diminished by p53 knock down. For cultures transfected with siRNA for p53, 24% of the cells showed nuclear p21 signal at 34 hours after Doxorubicin addition compared to over 90% for Doxorubicin treated cells with an intact p53 response (300 total cells were counted for each condition).

Lastly, we repeated the p53 knockdown, treated with Doxorubicin and continuously treated with 10μm Roscovitine, a Cdk2 inhibitor. Thirty-four hours later the incidence of extra centrioles was reduced from 27% to 9% **(Figure II-5B)**. Together these results indicate that duplication of disengaged centrioles in prolonged G2 after DNA damage is diminished by p53 mediated expression of p21 and the consequent inhibition of Cdk2 activity.

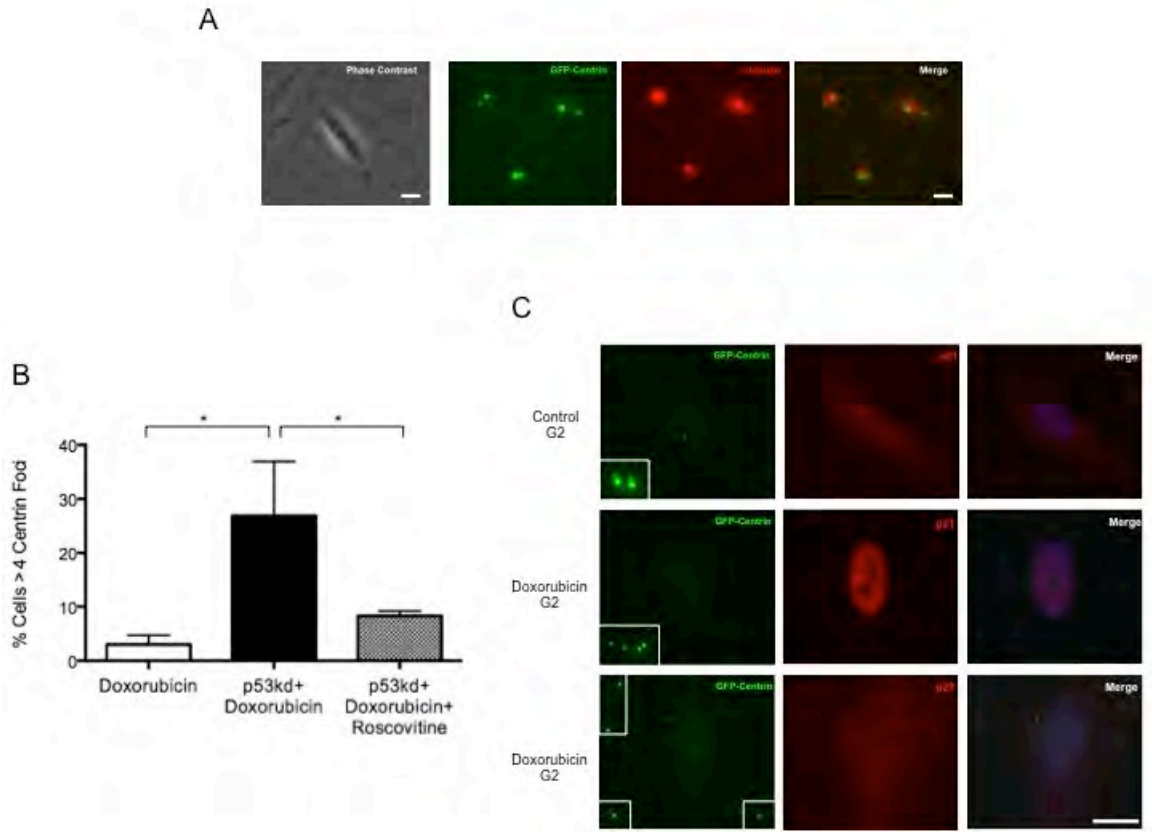

Figure II-5. Low incidence of centriole reduplication after DNA damage is due to p53-mediated inhibition of Cdk2 activity. (A) Correlative phase contrast/immunofluorescence images of a p53 knock-down cell 34hrs after Doxorubicin treatment showing extra centrioles. Phase contrast image was taken at 10X magnification and corresponding fluorescence images were taken at 100X magnification. GFP-centrin (green), γ-tubulin (red). Scale bars= 20μm and 1μm respectively. Fluorescence images are maximum intensity point projections from Z series images. (B) Incidence of cells with >4 centrin foci with indicated treatments 34hrs after Doxorubicin treatment. Histogram bars indicate the average from at least 3 experiments with 50 cells counted for each condition. Error bars are one standard deviation. *p≤ 0.05, determined by a two-tailed unpaired Student's t test. (C) Representative images of a control cell 14hrs after mitotic shake-off stained for p21 (upper row) and cells 72hrs after Doxorubicin treatment stained for p21 (middle row) and p27 (bottom row). Inserts are magnifications of all centrioles in each cell shown. GFP-centrin (green), p21 (red), p27 (red). Merge panels include DNA stained by Hoechst (blue). Scale bar=20μm. Images are maximum intensity point projections from Z series images.

Mitosis after DNA damage

Time lapse imaging of Doxorubicin treated cells revealed that even though most arrested in G2, 14% eventually enter mitosis within 72 hours after DNA damage. Since we observe a 52% incidence of centriole disengagement plus a 10% incidence of extra centrioles in G2 cells at this time, we wanted to know if cells that progressed into mitosis contained disengaged and/or amplified centrioles. We synchronized cultures in S phase with thymidine for 17hrs, and three hours after release pulsed with Doxorubicin. Since a small percentage of cells enter mitosis at variable times after DNA damage, we added Nocodazole 48 hours after the Doxorubicin pulse to accumulate in mitosis cells escaping from prolonged G2. Twenty-four hours later we fixed the cells and immunostained for γ-tubulin to complement the GFP centrin signal. We imaged 53 mitotic cells and found 12 cells with at least one pair of disengaged centrioles and 2 cells that contained supernumerary centrioles (6 centrioles). In 75 control mitotic cells all contained 2 pairs of engaged centrioles **(For complete breakdown see Table II-I)**. Since individual centrioles can organize spindle poles (Sluder and Rieder, 1985), 26% of the cells entering mitosis after DNA damage contained extra potential spindle poles.

	Cell Number	Centriole Configurations
Control	75	Two pairs of engaged centrioles
	0	One pair of disengaged centrioles
	0	Two pairs of disengaged centrioles
	0	More than four centrioles
DNA Damage	39	Two pairs of engaged centrioles
	5	One pair of disengaged centrioles
	7	Two pairs of disengaged centrioles
	2	More than four centrioles

Table II-I. Centriole configurations in control mitotic cells and cells that enter mitosis after DNA damage

Discussion

The radiation and radiomimetic drugs currently used to treat human tumors not only damage DNA in the cancer cells but also impact proliferating untransformed cells. Although centrosome amplification after DNA damage is well established for transformed cells, its occurrence in untransformed cells has been sparsely reported and not fully characterized (Kawamura et al., 2006; Sugihara et al., 2006; Saladino et al., 2009). We more thoroughly characterized the practical consequences of DNA damage for centrosome behavior in untransformed human cells. Our study differed from previous ones in at least two ways. First, we focused on centriole behavior, because after disengagement individual centrioles, when mature, can each organize a MTOC and at mitosis disengaged centrioles can organize multipolar spindles (Sluder and Rieder, 1985; Prosser et al., 2012). Second, we damaged DNA in synchronized cell populations to avoid the uncertainties in interpreting the responses of cells experiencing DNA damage at various points in the cell cycle.

Doxorubicin as used here damaged DNA in all cells and continuous time-lapse observations revealed that 86% of the cells arrested in G2 for at least 72 hours. In the G2 arrested populations, there was an increasing incidence of mother-daughter centriole disengagement that rose to 52% by 72 hours. On top of this we observed a 10% incidence of extra centrioles, consistent with values previously reported. Since all disengaged and reduplicated centrioles were

associated with γ-tubulin, the total incidence of functional centrosome amplification in prolonged G2 rose to 62% by 72 hours after DNA damage. This is substantially higher than the 5-15% incidence of centrosome amplification previously reported in studies on asynchronous untransformed cells after DNA damage (Kawamura et al., 2006; Sugihara et al., 2006; Saladino et al., 2009). The 10% incidence of extra centrioles we observed arose from reduplication during G2, not from cells that entered mitosis and failed cleavage.

The basis for centrosome amplification in transformed and untransformed cells has been uncertain. Proposed explanations include centrosome specific signaling, *de novo* centriole assembly, and centriole disengagement/reduplication due to G2 arrest (Inanc et al., 2010; Loffler et al., 2012, Prosser et al., 2012). Our results reveal that mother-daughter centriole disengagement after DNA damage is dependent on APC/C and/or Plk activities while the cells are arrested in G2. Blocking both activities almost completely suppressed centriole disengagement. Even though these activities normally act synergistically to disengage centrioles late in mitosis (Tsou et al., 2009), we found that either acting alone can eventually mediate disengagement after DNA damage. In the first 24 hours after DNA damage APC/C activity appears to be the primary driver of disengagement, but by 48 hours either APC/C or Plk activities can cause centriole disengagement. These observations are consistent with the report that without DNA damage either Plk or APC/C activity alone is sufficient to disengage centrioles during prolonged S or G2 phases, albeit more slowly than both acting

together (Hatano and Sluder, 2012, also see Loncarek et al., 2010 and Prosser et al., 2012). Which members of the Plk family participate in centriole disengagement after DNA damage is not certain. Plk1 activity is reported to be suppressed after DNA damage and Plk2 and Plk3 activities are reported to rise (Smits et al., 2000; reviewed in Bahassi, 2011). We did not observe obvious signs of possible *de novo* centriole assembly as indicated by the presence of supernumerary centrin foci lacking or weakly staining for γ-tubulin and C-Nap1 (Loffler et al., 2012). In our system all centrin foci showed robust co-localization of C-Nap1 and γ-tubulin.

In our experiments we noted a high incidence of centriole disengagement without reduplication; most cells contained just 4 separated centrioles and only 10% contained extra centrioles. This was curious because all the disengaged centrioles showed maturation characteristics, such as loss of SAS-6, the presence of CEP170, and accumulation of γ-tubulin, suggesting that they should in principle have been capable of reduplication (see Wang et al., 2011). Also, when these untransformed cells (without DNA damage) are arrested in G2 by inhibition of Cdk1 activity, the rate of centriole reduplication is ~60% (Loncarek et al., 2010). The results of our investigation of this issue indicated that a limit to reduplication of disengaged centrioles after DNA damage involves the p53 dependent expression of p21 resulting in the inhibition of Cdk2 activity. Knocking down p53 in Doxorubicin treated cells allowed an almost 10 fold increase in the incidence of centriole reduplication during prolonged G2, and this increase could

be reversed by inhibiting Cdk activity with Roscovitine. Cdk2 inhibition by p21 (reviewed in Maugeri-Saccà et al., 2013) is the likely limit for centriole reduplication, because inhibition of Cdk1 activity alone promotes supernumerary centriole assembly during G2 (Loncarek et al., 2010). Also, Cdk2 activity not only initiates normal centriole duplication (reviewed in Hinchcliffe and Sluder, 2002) but also is needed for centrosome amplification after DNA damage (Hanashiro et al., 2008; Bourke et al., 2010). p21 depletion in U2OS cells increases centrosome amplification after ionizing radiation (Shimada et al., 2011). An additional limit to centriole reduplication is suggested by reports that DNA damage leads to p53 mediated downregulation of Plk4, a kinase essential for the assembly of daughter centrioles (Li et al., 2005, Nakamura et al., 2013).

Putting these observations together, we propose that p53 mediated p21 expression after DNA damage arrests the cells in G2, a cell cycle phase in which natural increases in Plk and APC/C activities leads to the gradual disengagement of mother-daughter centrioles in most cells. However, the reduplication of these disengaged centrioles does not occur in most cases due to the inhibition of Cdk2 activity by p21. This explains why RO induced G2 arrest without DNA damage allows for a high incidence of centriole reduplication and why DNA damage in transformed cells with defects in the p53 – p21 pathways leads to a higher incidence of centriole reduplication than we find for untransformed cells.

We note that not all RPE1 cells exhibited centriole disengagement 72 hours after DNA damage. The gradual increase in the incidence of

disengagement from 24 to 72 hours suggests that the disengagement process is slow and had we followed cells longer, we perhaps could have seen a greater percentage of cells with centriole disengagement. We also found that ~10% of the cells showed centriole reduplication during prolonged G2 after DNA damage. The substantial prolongation of G2 in these cells speaks for p53 activity and one could thus ask why any showed centriole reduplication. We speculate that the inhibition of Cdk2 activity in those cells was not complete.

We were interested in whether DNA damaging therapies could have practical consequences for proliferating normal cells in cancer patients. Time-lapse observations of Doxorubicin treated cells revealed that ~14% eventually entered mitosis after spending substantial time in G2. We found that 26% of these cells went through mitosis with disengaged and extra centrioles, which would predispose them to assemble multipolar or transiently multipolar spindles. However, our time-lapse records showed that all cells in the end cleaved in a bipolar fashion. This is not surprising given that this cell type efficiently bundles centrosomes at mitosis (see Uetake and Sluder, 2004; Krzywicka-Racka and Sluder, 2011). Nevertheless, transient spindle multipolarity can lead to lagging chromosomes in anaphase and formation of micronuclei that do not fully replicate DNA, resulting in profound chromosome damage at mitosis (Ganem et al., 2009; Crasta et al., 2012). Therefore, DNA damage in proliferating normal cells during therapy with radiation or radiomimetics could lead to genomic instability through spindle pole amplification. Also, if the DNA damage compromises the p53– p21

pathways in any of these cells, they could tolerate mistakes and start to evolve transformed characteristics.

Acknowledgements

We thank Dr. Yumi Uetake, Dr. Anna Krzywicka-Racka, and Catherine Ward for useful suggestions and discussions. This work was supported by National Institutes of Health grant GM 30758 to G. Sluder.

Materials and Methods

Cell culture, drug treatment, and RNAi

HTERT-RPE1 cells stably expressing GFP-centrin1 were cultured in F12/DME (1:1) medium supplemented with 10% FBS and 1% Penicillin-Streptomycin. Cells were synchronized by mitotic shake-off or in G1/S-phase with 2.5mM thymidine (Sigma). To arrest cells in mitosis 1.6µm Nocodazole (Sigma) was used. Click-iT EdU assay (Invitrogen) was used to determine cells that had entered S-Phase. DNA damage was induced with a 1 hour 0.5µM Doxorubicin treatment. Plk1 activity was inhibited with 200nM BI2536 (ChemieTek); APC/C activity was inhibited with 12µM proTAME (R&D Systems), Cdk2 activity was

inhibited with 10μm Roscovitine (AG Scientific). The siRNA oligo duplex used to target human p53 was an ON-TARGETplus siRNA (J-003329-14, Dharmacon). A final concentration of 50nM siRNA was transfected using RNAiMAX (Life Technologies) according to manufacturers instructions. Fresh media was added 4 hours after transfection. Protocols for cell collection, siRNA transfection, drug treatments, and fixation times are shown diagrammatically at the top of corresponding figures and described in the text and figure legends.

Immunofluorescence

Cells were grown on glass coverslips and fixed in methanol at -20°C for >5 min. Primary antibodies used were: C-Nap1 (Santa Cruz; sc-135851) at 1:100; γH2AX (Millipore; #05-636) at 1:1000; γ-tubulin (Santa Cruz; sc-51715) at 1:200; SAS-6 (Santa Cruz; sc-81431) at 1:100; CEP170 (Invitrogen; #41-3200) at 1:500; p21 (AbCam; ab7960) at 1:200; p27 (Cell Signaling; #3698) at 1:1000. Secondary antibodies conjugated to AlexaFluor 594 (Life Technologies) were used at 1:1000. Hoechst 33258 (Sigma) was used to label DNA. Cell preparations were observed with a Leica DMR microscope equipped for phase contrast and epifluorescence. A 10X NA 0.3 or 100X NA 1.3 objective lens was used to collect Z stacks (0.2 μm steps) and the images shown are maximum intensity point projections series compiled with Slidebook software (Intelligent Imaging Innovations). Distances between centrioles were also measured using Slidebook software.

Live cell imaging

Cells were grown on glass coverslips and assembled into chambers containing F12/DME (1:1) medium as previously described (Uetake and Sluder, 2012). Groups of cells were circled on the coverslips with a diamond scribe and followed at 37°C with BH2 (Olympus), or DMEXE (Leica) microscopes equipped with phase-contrast optics using 10X objectives/ 0.3–0.32 NA. Image sequences were taken with Orca ER (Hamamatsu Photonics); Retiga EX (Qimaging, Corp.); or Retiga EXi Fast (Qimaging, Corp.) cameras. Images were acquired every 3 min with C-imaging software (Hamamatsu Photonics) and were exported as QuickTime videos using CinePak compression (Apple).

CHAPTER III: Comparative Phototoxicty of 488nm and 546nm Light on Cell Cycle Progression in Untransformed Human Cells

Abstract

We characterized practical aspects of using 488 and 546nm light for fluorescence observation of live untransformed human cells. Unlabeled mitotic cells were shaken off and given single 30 seconds to 2.5 minute irradiations in early G1 from a mercury arc lamp on a fluorescence microscope with GFP and RFP filter cubes. With 488nm light irradiations we observed a dose dependent decrease in the percentage of cells that progressed to mitosis and a slowing of the cell cycle for those that did enter mitosis. For 546nm light irradiations there was a 10-20% reduction in the percentage of cells entering mitosis but no strong dose dependency. For the longest irradiations, ~12% of cells died within 48 hours for 488nm light compared to only ~2% for 546nm. Cells expressing GFP-centrin1 or mCherry-centrin1 were more sensitive to 488 and 546nm irradiations respectively - fewer entered mitosis for each dose than unlabeled cells. For 488nm light irradiations of unlabeled cells, reducing the intensity tenfold or spreading the exposures out into a series of 10 second pulses at 1 minute intervals produced a minor and not consistent improvement in the percentage of the cells entering mitosis. However, reducing the oxidative stress on cells, either by culturing at ~3% oxygen or adding the water soluble reducing agent Trolox, provided a noticeable increase in the fraction of cells entering mitosis. Thus, for

live cell fluorescence studies, the relatively low phototoxicity of 546nm light suggests that use of RFP constructs is advantageous. For studies with GFP constructs reduction in oxidative stress can diminish the phototoxic effects of 488nm light.

Introduction

Live cell fluorescence observation of mammalian somatic cells is a powerful and widely used method to study cell structure, function, and physiology. Applications range from basic long-term time lapse cell observations to advanced methods including fluorescence recovery after photo-bleaching (FRAP), fluorescence resonance energy transfer (FRET), fluorescence lifetime imaging (FLIM**),** and ratiometric ion measurements (reviewed in Stephen and Allen, 2003; O'Connor and Silver, 2013; Cardullo, 2013; Chang et al., 2013). The excitation wavelengths used range from the near UV (340-360 nm) for cell permeable Ca++ indicating dyes to the far red (590-610nm) with some of the new generation of red fluorescent proteins.

A fundamental limitation for fluorescence observation of live cells has been the phototoxicity of the high intensity shorter wavelengths needed to image the commonly used fluorescent constructs such as EGFP (reviewed in Magidson and Khodjakov, 2013; Waters J 2013). Photodamage occurs through the light

induced formation of chemically reactive free radicals and formation singlet and triplet forms of oxygen (Zdolesk et al., 1993; Dixit and Cyr, 2003). The most obvious practical consequences of photodamage are bleaching of the fluorophore and cell death as seen by membrane blebbing, cell rounding, and apoptosis (Zdolesk et al., 1990; Dixit and Cyr 2003; Hoebe et al., 2007; Kuse et al., 2014). Paradoxically, obvious changes in cell morphology and cell death may be the kindest manifestation of photodamage. One knows right away that there is damage that has impacted the experimental results. A more pernicious problem occurs when the excitation light diminishes cell viability, alters cell physiology, and stresses the cell thereby making it susceptible to additional experimental stressors. Well before the cell visibly dies or the fluorophore bleaches, the cell can sustain substantial functional damage, something that may not be evident until later if the observations last long enough (see Magidson and Khodjakov, 2013).

Stress is additive and stresses that are singly of little consequence can act additively to significantly impact cell physiology and behavior. Consequently, the interpretation of the experimental results is greatly complicated by the problem that one cannot fully know if the response of the cell is due to photodamage or the experimental perturbation or both. For example studies provided seemingly compelling evidence that the removal of the centrosome from mammalian cells causes a G1 cell cycle arrest (Hinchcliffe et al. 2001; Khodjakov and Rieder, 2001). However, a later investigation demonstrated that this arrest resulted from

the combined stresses of centrosome removal, culture conditions, and microsurgery or blue light exposure in conducting the laser ablations of GFP centrin tagged centrioles (Uetake et al., 2007). Other examples of functional photodamage, short of cell death, include the finding that illumination of mid-prophase PtK cells with 488nm light leads to chromosome decondensation and the return of cells to a G2-like state (Khodjakov and Reider, 1999). Also, exposure to blue light can markedly diminish the proliferative capacity of yeast and embryonic *C. elegans* cells (Carlton et al., 2010; Tinevez et al., 2012).

In practice photodamage may not always be an issue for short-term observations involving few images. However, it is a serious problem for applications involving long-term observations with many images, particularly when each time point requires taking a Z-stack and/or if more than one fluorescent protein is being visualized. Further, due to imprecise hardware synchronization between the shutter and camera, actual exposure times are often longer than what is set. This can be especially troublesome when many Z-stacks are recorded for multiple colors (see Magidson and Khodjakov, 2013). Importantly, in all applications photodamage begins even before the imaging sequence begins; scanning the slide, identifying a cell of interest, and bringing the structures of interest to focus in the center of the field can require a minimum of several seconds – the equivalent of many imaging exposures.

Traditionally the most commonly used excitation wavelengths are blue (488nm) for EGFP and green (~546nm) for the RFPs. Although the damaging

effects of blue light are well recognized (reviewed in Waters, 2013), the extent to which green light damages mammalian somatic cells has not been systematically tested. Green light has been generally assumed to be benign, but, should this not be the case, investigators will have to evaluate whether the use of RFP constructs is worthwhile given their lower brightness relative to EGFP and the consequent need for longer excitations per image.

Our study had two objectives. First, we systematically characterized the relative phototoxicity of blue (488nm) light on the cell cycle progression of untransformed human cells expressing and not expressing fluorescent proteins. This result provided us with the basis against which to directly compare the effects of equivalent exposures, in both watts and total photons, of green (546nm) light on cell cycle progression. We chose these wavelengths because they are widely used for work with GFP and RFP and can serve as a proxy for the phototoxicity of similar wavelengths used to excite other fluorescent proteins, such as CFP (439nm) and YFP (514nm).

Second, we tested the efficacy of three stratagems that have or could be used to mitigate the phototoxicity of 488nm blue light in imaging. We examined the reciprocity relationship for photodamage between intensity and exposure duration to test the intuitive notion that lower intensities for longer times allow cells to some extent buffer the photodamage (discussed in Swedlow and Andrews 2005; Magidson and Khodjakov, 2013). We also tested if there is functionally significant leakage of short wavelengths through the excitation filter.

Although modern excitation filters for 488nm excitation commendably provide ~5 OD suppression of wavelengths below 488nm, the high pressure mercury arc lamps in widespread use have extremely strong emission lines at 410, 365, and 366nm. Lastly, we tested if reduction of oxidative stress could improve the cell's tolerance for blue light.

Results

Experimental system:

All work was performed with hTERT – RPE1 cells. These untransformed human cells have intact cell cycle checkpoints including a normal p53 response to damage. In response to various experimental perturbations these cells behave in a qualitatively identical fashion to primary human cells (Uetake et al., 2004, 2007, 2010). We did not use cancer cell lines, all of which have suites of defects that could in principle mask or alter their sensitivity and response to photodamage.

To assay for photodamage we used the timing and extent of interphase cell cycle progression because this is a more sensitive assay than overt cell death. We shook off mitotic cells and plated them on coverslips. Two hours later (early G1) marked fields of cells were irradiated with one of several regimes of blue (488nm) or green (546nm) light and then continuously followed with phase contrast optics by time-lapse video microscopy with shuttered green light. Under

our observation conditions control RPE1 cells proliferate to confluency and remain viable for at least 13 days.

Single dose irradiations of 488nm and 546nm light

We first tested the effects of single irradiations of blue or green light ranging from 0.5 – 2.5 minutes on unlabeled cells. Light was delivered through a conventional epifluorescence pathway with a 100W high-pressure mercury lamp and Leica L5 or Leica Red-GFP filter cubes **(See Figure III-1A,B**) and a 20X, 0.4 NA objective. Light intensities at the specimen plane were 14mW/mm^2 for 488nm and 21mW/mm^2 for 546nm light **(See Table III-1 for specifics)**. Irradiated and same preparation control fields were continuously followed using shuttered transmitted green light for 48 hours (~2 normal cell cycles). We determined how many cells progressed into mitosis, and if so, the total time each took to reach mitosis.

For 488nm light irradiations we observed a dose-dependent decrease in the percentage of cells that progressed into mitosis compared to control cells. Also, those that did reach mitosis took longer to do so **(Figure III-2A)**. These results are plotted as the total percentage of cells that had entered mitosis as a function of time after the irradiation, with every point on the curve being a cell that entered mitosis. In addition, cells that arrested for 48hrs were positive for nuclear p21 **(Figure III-3)**. For the 1min and longer irradiations, some cells became less flat than the controls and showed reduced motility for up to 20

Equipment/Parameters	Description
Microscope	Leica DMRE
Light Source	100W High Pressure Mercury Arc Lamp (OSRAM)
Objectives	Irradiate: Leica N Plan, 20X, 0.40NA Film: Leica HC Plan Fluotar, 10X, 0.30NA
Filter Cubes	Leica L5: Excitation= BP 480/40 Leica Red-GFP: Excitation= BP546/12
Light Intensities	Blue: 14mW/mm^2 Green: 21mW/mm^2
Epi-illumination Field Diaphragm	Set just inside field of view
Epi-illumination Condenser Diaphragm	Set 67% open

Table III-1. Description of the equipment and parameters used for light irradiations

A

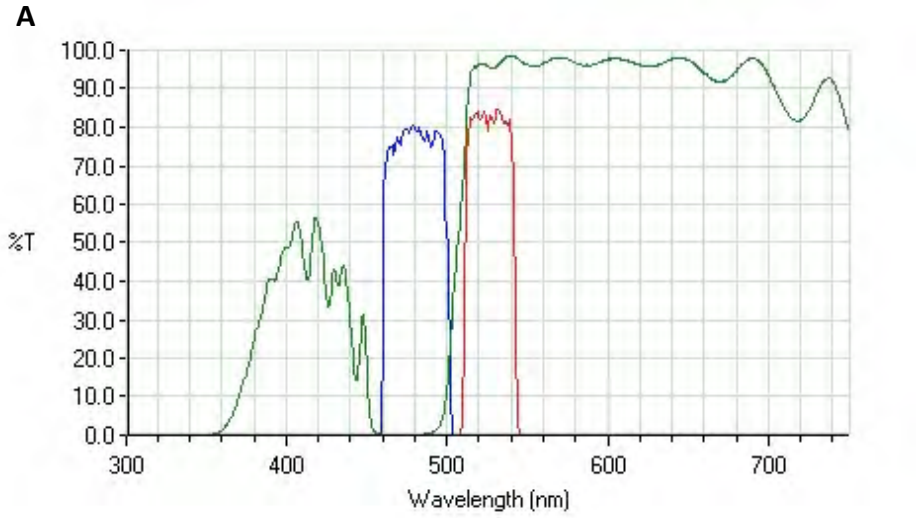

B

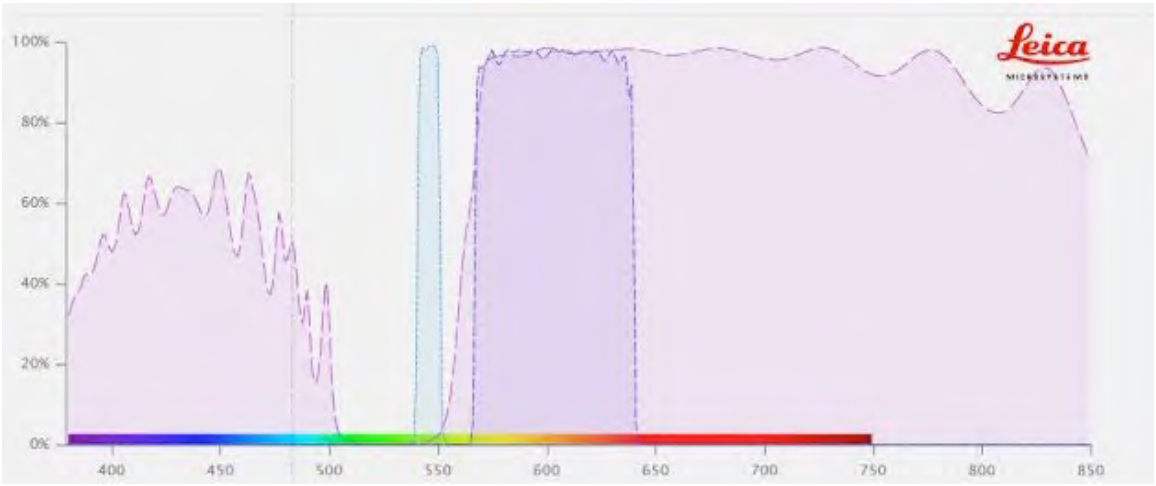

Figure III-1. Spectral Characteristics of Filter Cubes. (A) Graph displaying %transmission vesus wavelength for the L5 filter cube. Green line represents the dichroic mirror, the blue line represents the excitation filter, and the red line represents the emission filter. (B) Graph displaying %transmission vesus wavelength for the Red-GFP filter cube. The light purple dashed line represents the dichroic mirror, the blue line represents the excitation filter, and the dark purple dotted line represents the emission filter. Graphs are courtesy of Leica Microsystems.

hours. After that time they flattened, resumed normal motility, and some eventually entered mitosis. We also found a dose-dependent increase in the percentage of cells that died, going up to an average of 12% for the 2.5min irradiations **(Figure III-2D)**. For 546nm light irradiations, we found a 10-15% reduction in the number of cells eventually reaching mitosis, but no strong dose dependency **(Figure III-2B)**. For the cells that did not enter mitosis, we did not observe any changes in cell flattening or motility as was the case for the 488nm irradiations. For the longer irradiations with green light only 2% of the cells died **(Figure III-2D).**

Since we used different watts per mm^2 for the two wavelengths and blue light is more energetic per photon than green light, we expressed the exposures in terms of total number of photons delivered per unit area for both wavelengths. Percent cells that entered mitosis within 48 hours for total photon doses are shown in **Figure III-2C**. For 488nm light exposures there is a clear dose dependency for the extent of interphase arrest. For 546nm light irradiations, there is a modest but roughly constant reduction in the percentage of cells entering mitosis.

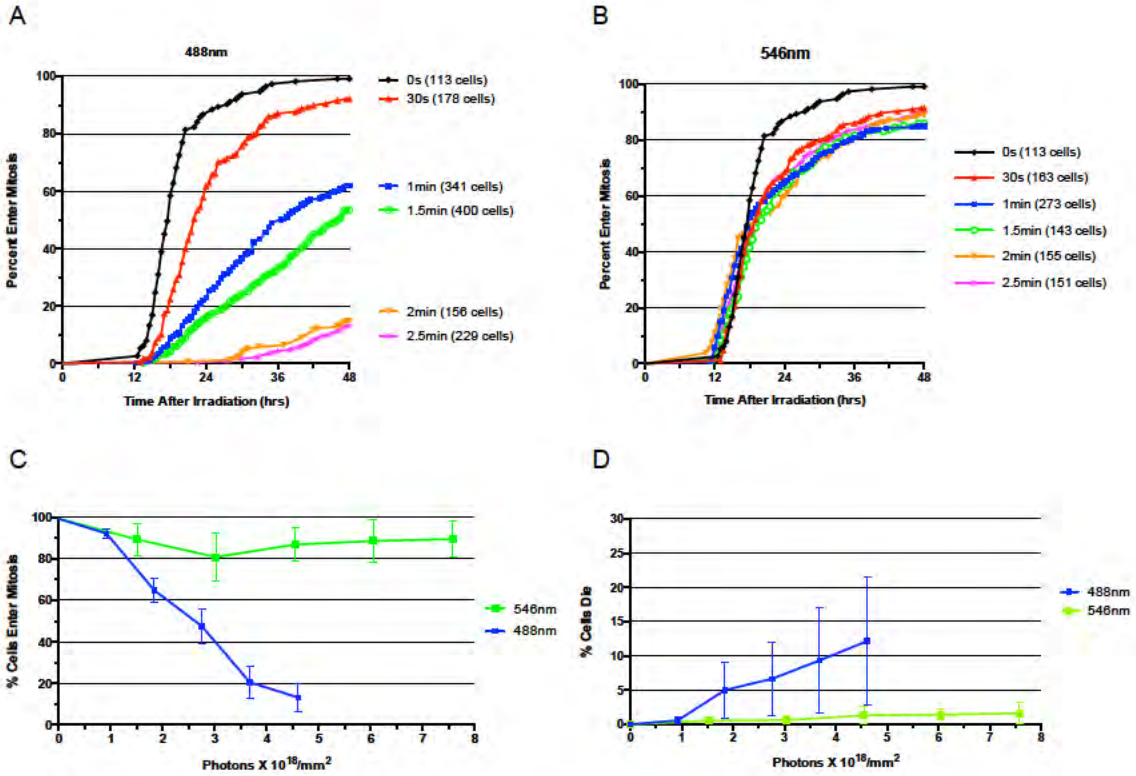

Figure III-2. Effects of single 488nm and 546nm light irradiations on G1 to mitosis progression for unlabeled cells. Fields of G1 cells were irradiated for the indicated durations and continuously followed for 48 hours. (A) (488nm, 14mW/mm2) and (B) (546nm, 21mW/mm2); percentages of the irradiated populations that entered mitosis are shown as a function of time after the irradiation. Each point represents a cell that entered mitosis. Each line is the combined data from 3 or more experiments and total cells followed for each irradiation regime are given next to each curve. C.) Percentage of cells that entered mitosis by 48hrs as a function of total 488nm and 546nm photons/mm2 administered at the specimen plane. D.) Percent cell death within 48hrs after each 488nm and 546nm light irradiation as a function of total 488nm and 546nm photons/mm2 administered at the specimen plane. For C and D each point represents the average from at least 3 experiments and error bars depict SEM.

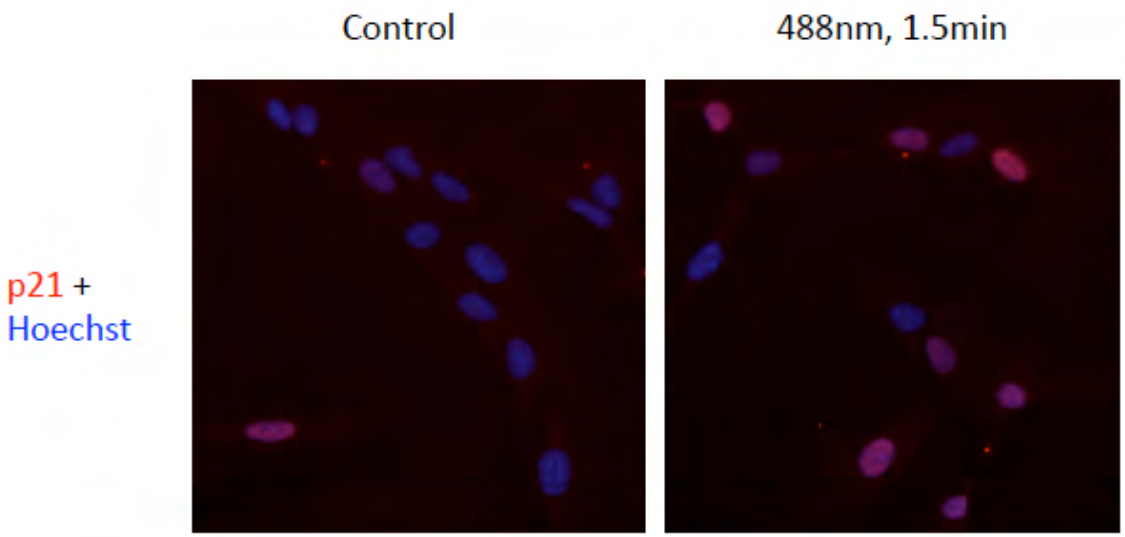

Figure III-3. **488nm Irradiations lead to p21 nuclear localization.** Populations of cells were marked and irradiated with 488nm light for 1.5min. After 48hrs, cells were fixed and stained for p21 and Hoechst. The percentage of cells positive for nuclear p21 are listed for the irradiated and control cells. At least 150cells were counted for each condition.

Fluorescent proteins and sensitivity to blue or green light

The generation of reactive oxygen species (ROS) is believed to play a role in causing phototoxicity (Zdolesk et al., 1990; Zdolesk et al., 1993; Dixit and Cyr, 2003). Dixit and Cyr (2003) reported that the presence of a fluorescent protein enhances the amount of ROS in tobacco cells exposed to 546nm light. Thus, we tested if expression of fluorescent proteins influences the sensitivity of cells to blue or green light.

We repeated the 30s, 1min, and 1.5min single 488nm irradiations using RPE1 cells stably expressing GFP-centrin1. Centrin1 is present throughout the cytoplasm, and a small percentage is concentrated in the distal lumen of centrioles throughout the cell cycle (Piel et al., 2001). For unirradiated cells 99% of wild type and GFP centrin1 expressing cells entered mitosis with essentially the same kinetics **(Figure III-4A)**. For the 30s irradiation 10% fewer GFP centrin1 expressing cells entered mitosis in 48 hours than the unlabeled cells (Figure 2A). We did not observe a difference for the 1min irradiations, but at 1.5min, 25% fewer GFP centrin1 expressing cells entered mitosis compared to unlabeled cells. The same experiment was conducted with 546nm irradiated m-Cherry centrin1 expressing cells. Ninety percent of the unirradiated cells entered mitosis in 48 hours **(Figure III-4B)**. This suggests that m-Cherry centrin1 expression *per se* is a stress. Nevertheless, we observed a modest light dose dependent decrease in the percentage of cells that entered mitosis **(Figure III-**

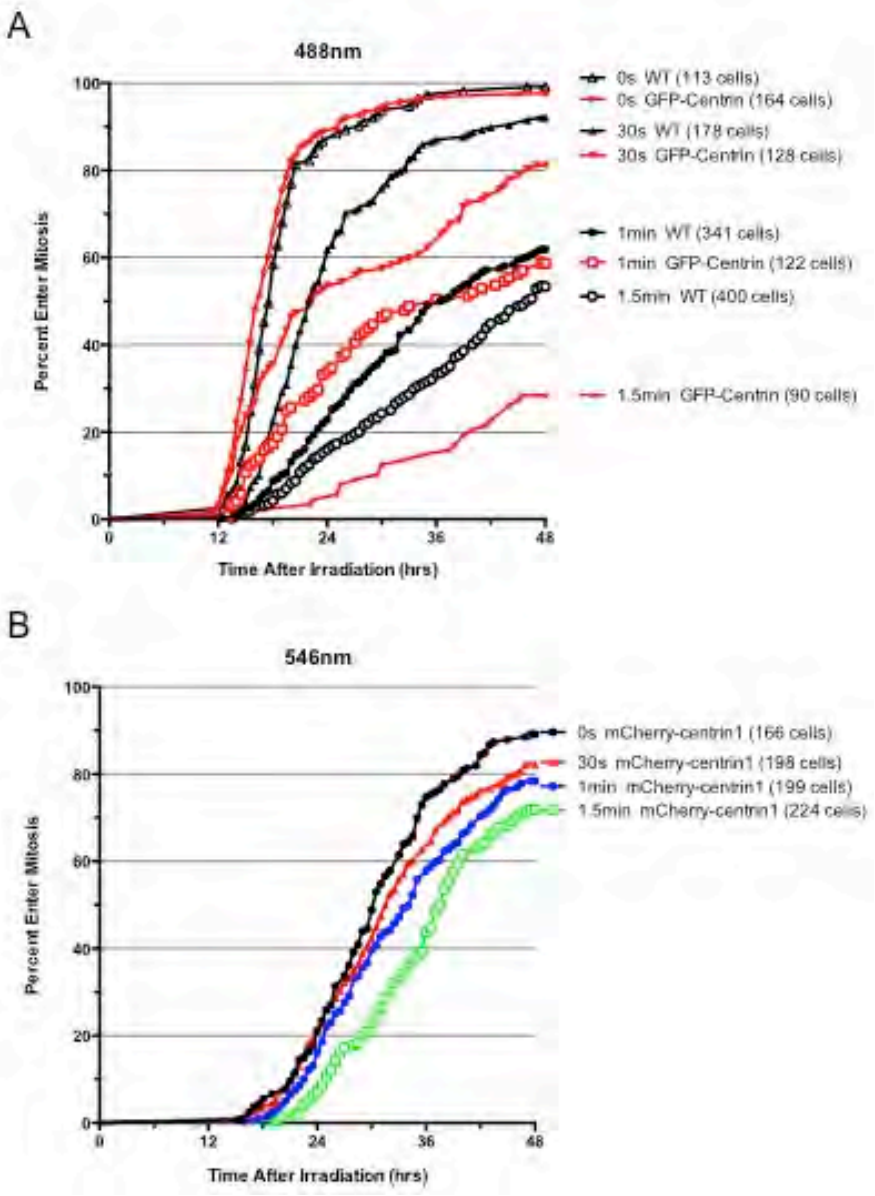

Figure III-4. Effects of single 488nm and 546nm light irradiations on G1 to mitosis progression for cells expressing fluorescent proteins. Percentages of the irradiated populations that entered mitosis are shown as a function of time after the irradiation. A.) The percentage of the irradiated populations that entered mitosis as a function of time after 488nm irradiations are shown in black for the unlabeled cells and in red for the cells expressing GFP-centrin1. B.) Percent entry into mitosis with time after 546 nm irradiations is shown in black for the unlabeled cells and in red for the cells expressing mCherry-centrin1. Each line is the combined data from 3 or more experiments and total cells followed for each irradiation regime are given next to each curve.

4B), something not seen to this extent for unlabeled cells exposed to green light **(Figure III-2B)**.

Reciprocity relationships

The possibility that spreading light exposures out over longer times allows cells to some extent buffer the photodamage has been an attractive notion (discussed in Swedlow and Andrews, 2005; Magidson and Khodjakov, 2013). Support for this notion comes from the report of Dixit and Cyr (2003) that reducing 488nm light intensity and increasing exposure times led to a reduction in mitotic arrest and cell death for tobacco cells. We used two strategies to slow the delivery of the 488nm light without diminishing the total doses given. First, we broke the full intensity irradiations into a series of 10 second exposures separated by one minute, similar to what would happen with the repetitive acquisition of Z-stacks of 20 images each with a 500 millisecond camera exposure. Second, we used single irradiations at 10% intensity for correspondingly longer times.

For the following experiments we used unlabeled cells exposed to 488nm light. First we spread the 30s, 1min, and 1.5min total 488nm irradiations into a series of 10 second pulses, each administered every minute. For the 30 second total exposures, the same percentage of the cells entered mitosis by 48 hours for the population given pulses as did for the single, full time irradiations **(Figure III-**

5A). We note that some cells in the populations exposed to pulses entered mitosis sooner than their counterparts given a single longer irradiation. For the 1 minute total exposures spread out into pulses, the kinetics for entry into mitosis was slightly faster and by 48 hours 10% more cells entered mitosis than populations given a single irradiation. For the 1.5 minute total exposures, those populations given pulses entered mitosis slightly slower than their single dose counterparts but by 48 hours similar percentages had entered mitosis. Thus, spreading out the exposure to 488nm irradiation into a series of full strength pulses provides at best a modest improvement in cell viability.

To test if longer but lower intensity single irradiations moderated the phototoxic effects of 488nm light we cut the incident intensity to 10% with a neutral density filter. Unlabeled cells were given single correspondingly longer exposures so as to maintain the same total light dosages as the 30 second, 1 minute, and 1.5 minute irradiations used in the experiment plotted in **Figure III-2A**. As shown in **Figure III-5B**, we found no great or consistent improvement in the percentage of cells entering mitosis by 48 hours. Thus, longer but lower intensity exposures did not mitigate the phototoxicity for 488nm light.

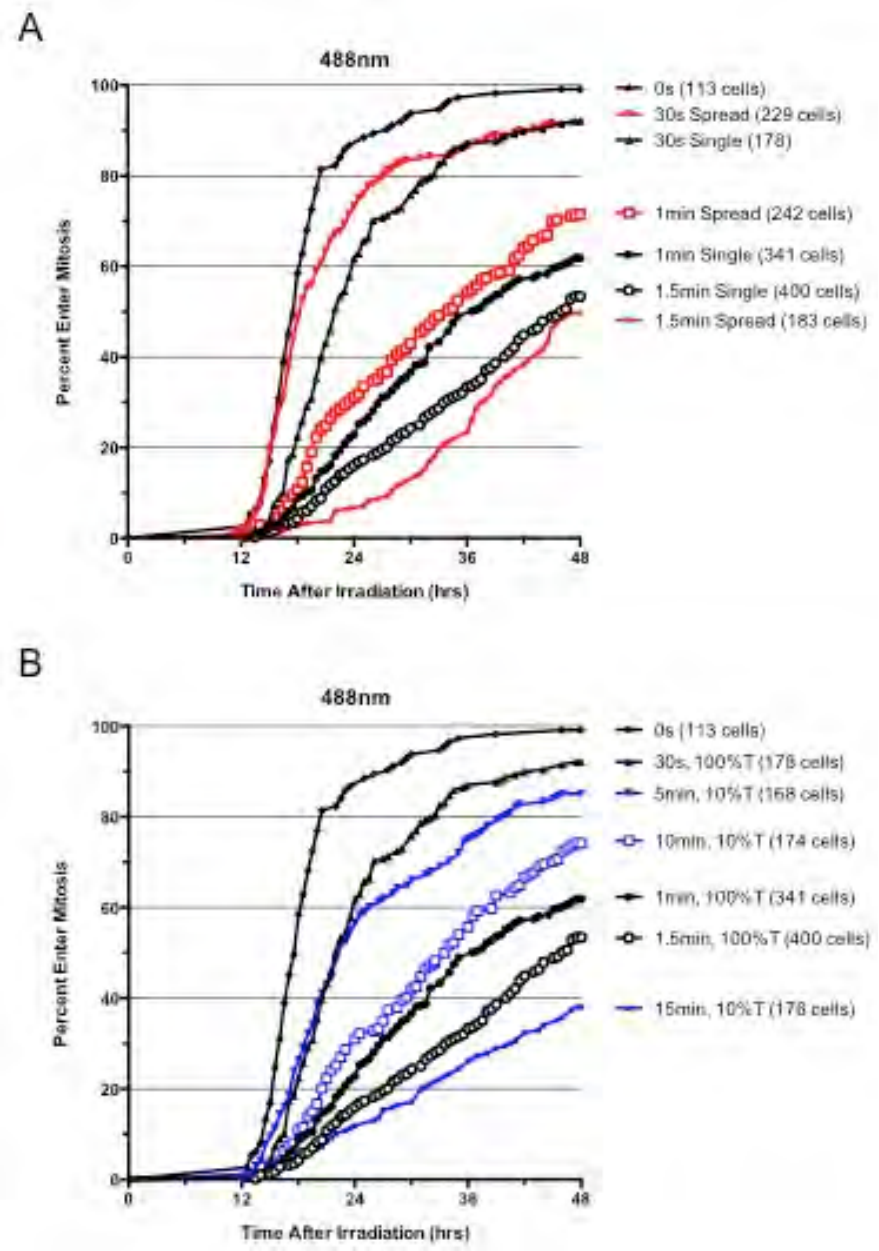

Figure III-5. Effects of prolonging the delivery of 488nm irradiations on G1 to mitosis progression for unlabeled cells. A.) The total doses were spread out into a series of 10 second, full intensity pulses delivered one minute apart. The percentage of the irradiated populations that entered mitosis as a function of time after single irradiations are shown in black and in red for the same doses spread out into pulses. B.) The total doses were delivered as single 10X longer irradiations of 10% intensity– blue curves and single full intensity irradiations – black curves. Each line is the combined data from 3 or more experiments and total cells followed for each irradiation regime are given next to each curve.

Additional attenuation of short wavelengths

High-pressure mercury arc lamps have strong emission lines at 365-366, and 405 and 436 nm. The 365 - 366 nm line is ~30 times brighter than the 488nm peak and the others are ~20 times brighter. Although modern 488nm excitation filters provide ~5 OD suppression of wavelengths below 488nm, we tested if putative leakage of these short wavelengths through the 488 and 546nm excitation filters participated in producing phototoxicity. We added a long-pass filter into the light path that adds 4 OD suppression below <430nm **(Figure III-6C)** and repeated the single 488nm and 546nm irradiations. Since the long-pass filter reduced watts per mm2 at the specimen plane for each wavelength, we expressed the exposures in terms of total number of photons per unit area delivered. Addition of the long pass filter produced no improvement in the percentage of cells entering mitosis by 48 hours for any of the 488nm exposures and at best a slight improvement for the 546nm irradiations **(Figure III-6A,B)**. Thus, addition of a long pass filter to the fluorescence-illuminating pathway is not detrimental, but does not represent a practical way to mitigate the phototoxicity of 488nm light.

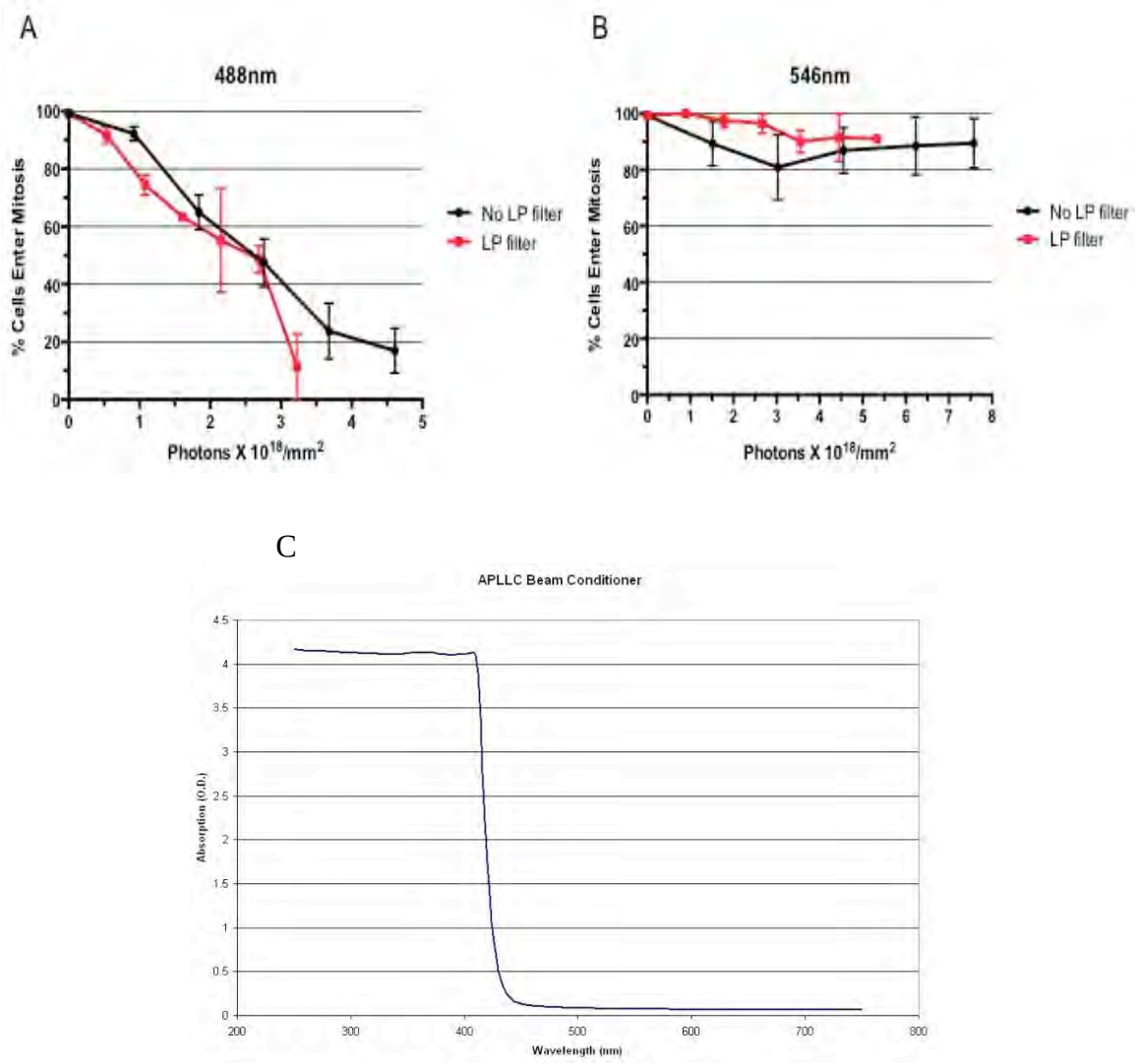

Figure III-6. Introduction of a long pass filter into the irradiating pathway to test for phototoxic consequences of putative leakage of short wavelengths through excitation filters. A.) Percentage of cells that entered mitosis by 48hrs as a function of total 488nm photons/mm2 administered at the specimen plane with (red) and without (black) the long pass filter. B.) Percentage of cells that entered mitosis by 48hrs as a function of total 546nm photons/mm2 administered at the specimen plane with (red) and without (black) the long pass filter. Each point represents the average from at least 3 experiments and error bars depict SEM. C.) Graph displaying the absorption in O.D.'s for the long-pass filter as a function of wavelength. Graph is courtesy of Paul Goodwin (API).

Reducing oxidative stress

The production of ROS can lead to oxidative stress and damage living cells. Heretofore, all of our experiments were conducted with cells cultured at atmospheric oxygen level (~20%), which is higher than the physiologic levels within mammalian organisms (3-14%), depending on the tissue (reviewed in Sen and Roy, 2010). Thus, we used two ways to reduce oxidative stress in unlabeled cells and tested if this reduced the phototoxicity of 488nm light. We equilibrated cells and the culture medium with 3% oxygen, 5% CO2, and 92% nitrogen. Mitotic shake off cells were plated on coverslips and later mounted in observations chambers under these conditions. Marked fields were either given single 1 or 1.5 minute irradiations with 488nm light or not irradiated to serve as a control. Shake-off cells (no light) grown at low 3% oxygen exhibited similar cell cycle dynamics as cells grown at atmospheric oxygen. For the 1 minute irradiations we found that 27% more cells entered mitosis than those irradiated under atmospheric oxygen levels **(Figure III-7A)**. For the 1.5 minute irradiations 25% more cells progressed to mitosis than those irradiated under standard atmospheric oxygen levels **(Figure III-7B)**. Nevertheless, reduced oxygen levels did not completely mitigate phototoxic consequences of 488nm light. Approximately 7% fewer cells entered mitosis for the 1.5 minute irradiations than for the 1 minute irradiations **(Figure III-7A versus III-7B)**. Our second strategy was to continually treat cells grown at atmospheric oxygen level with 500um Trolox, a water-soluble antioxidant. For the 1min irradiations almost all cells

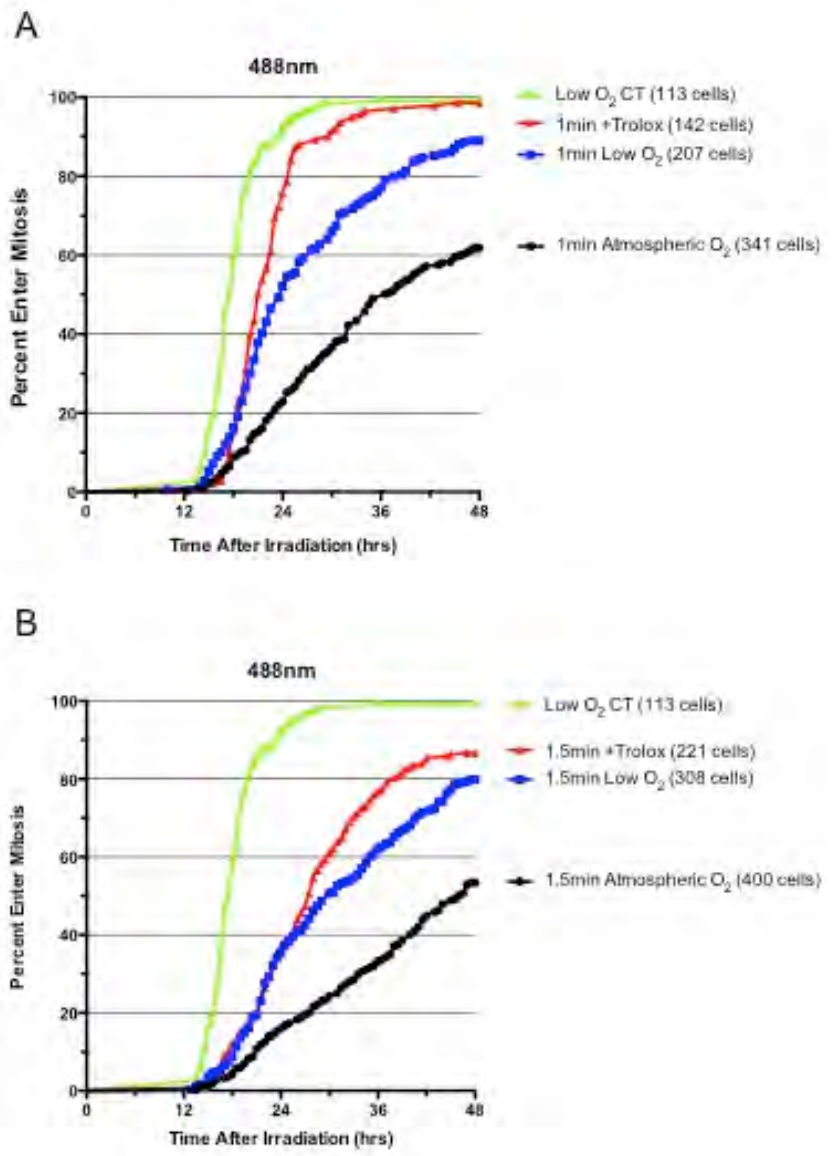

Figure III-7. Effects of 488nm light irradiations on G1 to mitosis progression under conditions of reduced oxidative stress. Percentages of the irradiated populations that entered mitosis are shown as a function of time after the irradiation. A.) Comparison of populations receiving single 1 minute irradiations under atmospheric (20%) oxygen levels plus 500uM Trolox (red), under ~3% oxygen levels (blue), under atmospheric oxygen levels (black), and under 3% oxygen levels with no light (green). B.) The results of the same experiment with 1.5 minute single irradiations. Each line is the combined data from 2 or more experiments and total cells followed for

progressed into mitosis, a 38% increase over cells irradiated without Trolox. For the 1.5 minute irradiations 85% of the cells progressed to mitosis, approximately a 35% improvement. Together, these results indicate that reduction in oxidative stress reduces the phototoxic consequences of 488nm light exposures, but does not eliminate it.

Discussion

Beyond the photobleaching of fluorescent proteins, a major limitation for the repetitive imaging of living cells has been the degradation of cell viability. This is particularly a problem when the cells do not immediately die, but their cellular function is compromised but not obviously so in the experimental context. The purpose of our study was to provide practical assessment of the phototoxicity of 488 and 546nm light on untransformed human cells that have the normal suite of checkpoints and damage responses. We also tested strategies that have or could be used to mitigate phototoxicity. We used blue and green light because they are commonly used to image cells expressing GFP or RFPs and we expect that these wavelengths can be used as a proxy for similar wavelengths used to excite other fluorescent proteins such as, ECFP, EYFP, and dsRed. As a functional measure for phototoxicity we used the cell cycle arrest because it a more sensitive assay than overt cell death.

488nm light

It comes as no surprise that 488nm light is phototoxic to living cells as seen here as a dose dependent reduction in the percentage of the cells that enter mitosis and the slower progression through interphase for those that do reach mitosis. Single 2.5 minute irradiations of unlabeled cells led to an interphase arrest of 90% of the cells. There was a dose dependent increase in the incidence of cell death, reaching 12% for the longest exposures. We also found that expression of GFP-centrin 1 sensitized cells to 488nm light exposures. For example, 1.5 minute irradiations reduced the percentage of cells entering mitosis from 53% for unlabeled cells down to 28% for GFP-centrin 1 expressing cells. In a broader sense this finding suggests that investigators should follow only those cells that express low levels of the fluorescent-tagged proteins even though the distribution of the tagged proteins may be harder to image.

It has long been suspected that longer lower intensity irradiations of 488nm light promote cell viability by allowing the cell time to buffer the phototoxic reactions to some extent (Dixit and Cyr, 2003; discussed in Magidson and Khodjakov, 2013). However, for the range of light doses we used in G1 we found at best a slight and not consistent reduction in phototoxicity when total light doses were spread out as a series of 10 second pulses given a minute apart or a ten fold reduction in the excitation intensity for single exposures. Thus, it

appears that there is little to be gained by slowing the delivery of the 488nm light; total dose is what matters.

We also tested anecdotal reports that the use of a long pass filter in the illumination pathway promotes cell viability by suppressing the putative leakage through the excitation filter of the intense mercury arc emission lines at wavelengths less than 430 nm. The possible value of this test is supported by the fact that the 365, 366, and 410 nm emission lines individually are up to approximately 30 times as intense as the 488nm emission peak. However, we found no significant reduction in phototoxicity with the presence of a long pass filter that provides a ~4 OD's of additional suppression of these short wavelengths.

The one experimental stratagem that improved cell viability after 488nm light exposure was reducing the oxidative stress to the cells. The generation of reactive oxygen species (ROS) is believed to be the driving force is causing phototoxicity (Zdolesk et al., 1990; Zdolesk et al., 1993; Dixit and Cyr, 2003). Cells are almost universally cultured under atmospheric conditions (~20% or a pO_2 of 140 mm Hg at sea level). This is higher than the *in vivo* mammalian levels, which range from 3-14% depending on the tissue (reviewed in Sen and Roy, 2010). We found that reducing oxygen levels in the observation chambers to ~3% allowed substantially more cells to progress to mitosis for two exposures to 488nm light. Trolox, a water-soluble antioxidant, has been used to reduce photobleaching of fluorescent proteins (discussed in Swedlow and Andrews,

2005; Waters, 2013). Here we tested if it could also diminish the phototoxicity of 488nm light for cells grown under atmospheric conditions. We found that inclusion of 500uM Trolox in the culture medium noticeably increased the percentage of cells that progressed to mitosis at atmospheric oxygen levels. Indeed, Trolox was slightly better than low oxygen levels in promoting cell viability. Thus, long term imaging of cells expressing GFP, or fluorescent proteins with similar excitation wavelengths, should substantially benefit from culturing the cells at reduced oxygen levels or the addition of Trolox to the culture medium.

546nm light

Compared to 488nm light, 546nm light is far less phototoxic for unlabeled cells. We observed a 10–15% reduction in the percentage of cells entering mitosis after all irradiations and no clear dose dependency. Also, only 2% of the cells died after the longest irradiations. When the doses are expressed as the total number of photons delivered per unit area of the specimen plane, unlabeled cells well tolerated just over 50% more incident 546nm photons than found for highest dose of 488nm light. However, the expression of a RFP construct sensitized the cells to 546nm irradiation. Cells expressing mCherry-centrin1 showed a modest dose dependent reduction of cells entering mitosis suggesting a participation of the fluorescent protein in phototoxic reactions.

These results reveal that 546nm light is a far less toxic wavelength for imaging than 488nm light. This means that the use of RFP constructs in repetitive imaging should allow better cell viability than the use of GFP constructs. This could translate into more frequent imaging and longer film runs. However, 546nm light is not entirely safe; there is some functional phototoxicity, particularly when the cell expresses a RFP construct. Additionally, the investigator will have to take into account that RFPs are generally less bright than GFP and consequently may require longer excitation exposures for each image.

Acknowledgements

We thank Dr. Yumi Uetake and Dr. Anna Krzywicka-Racka for useful discussions and suggestions. We also thank the UMass Biomedical Imaging group for the use of their photometer and useful discussions. This work was supported by National Institutes of Health grant GM 30758 to G. Sluder.

Materials and Methods

Cell culture, treatment, and immunofluorescence

hTERT-RPE1-WT cells and hTERT-RPE1 cells stably expressing GFP-centrin1

or mCherry-centrin1 were cultured in F12/DME (1:1) medium supplemented with 10% FBS and 1% Penicillin-Streptomycin. For noted experiments, 500um Trolox (Sigma) was added to culture media one day before mitotic shake-off and re-added immediately after shake-off. All cells were grown at atmospheric oxygen (~20%) unless specified. For low oxygen culture conditions, cells were grown and maintained in a modular incubator chamber (Billups-Rothenberg) flushed with a custom gas mixture containing 3% oxygen, 5% CO2 and 92% nitrogen one day before mitotic shake-off and re-flushed immediately after mitotic shake-off. For immunofluorescence experiments cells were grown on glass coverslips and fixed in methanol at -20 degrees celsius for >5 minutes. The primary antibody p21 (AbCam) was used at 1:200. Secondary antibodies conjugated to AlexaFluor 594 (Life Technologies) were used at 1:1000. Hoechst 33258 (Sigma) was used to label DNA.

Light irradiations and live-cell imaging

Mitotic shake-off cells were grown on glass coverslips and assembled into observation chambers containing F12/DME (1:1) medium as previously described (Sluder et al., 2005). Groups of cells were circled on the coverslips with a diamond scribe. Two hours after shake-off blue (488nm) or green (546nm) light was delivered to cells through a conventional epifluorescence pathway, with a 100W high-pressure mercury lamp (OSRAM) and Leica L5 or Leica Red-GFP filter cubes and a 20X, 0.4 NA objective. Multiple fields of cells

were followed at 37°C with DMRE or DMIRE2 (Leica) microscopes equipped with phase-contrast optics using 10X/0.3 NA objectives using shuttered green light. Image sequences were taken with Orca ER (Hamamatsu Photonics) cameras. Images were acquired every 3min with C-imaging software (Hamamatsu Photonics) and were exported as QuickTime videos using CinePak compression (Apple).

Light intensity and photon determination

Light intensities for each wavelength were determined using a Newport 1916-C power meter. The detector was placed at the specimen plane under the 20X objective and intensities were measured in watts. Light output was regularly monitored to ensure light output was consistent between experiments. For total photon determination we calculated the energies from each peak wavelength ($4.07X10^{-19}$J/photon for 488nm, $3.64X10^{-19}$J/photon for 546nm) using $E=hc/\lambda$. We then divided the power measurements by the corresponding energies to determine photons/s. This number was then multiplied by the total seconds of each exposure to determine total photons administered.

CHAPTER IV: DISCUSSION AND FUTURE DIRECTIONS

The work presented in this thesis covers two separate studies on the consequences of cellular damage. Together, my work demonstrates the importance of proper centriole regulation after DNA damage in untransformed human cells, suggests a connection between DNA damaging cancer therapies and the development of further transformation **(Chapter II)**, and provides practical assessments of microscopy induced photodamage and potential ways it can be mitigated **(Chapter III)**. Here, I have discussed the current understanding of centriole behavior after DNA damage, the connection between centrosome amplification and cancer, and the importance of recognizing microscopy induced phototoxicity. Further, I propose questions that still remain and suggest possible work that can be done to continue progress in each of these areas.

DNA damage and centrosome amplification

It is well established that DNA damage leads to centrosome amplification in transformed cell lines. Interestingly, the reported incidence of centrosome amplification in untransformed cells was much less than reports for transformed cells. However, the findings in untransformed cells were sparsely reported and not completely understood. We were particularly interested in better characterizing centriole behavior after DNA damage in untransformed human

cells, as well as, determining the reason for the large difference in centrosome amplification between untransformed and transformed cells.

Our findings that only 10% of cells contained centrosome amplification after treatment with Doxorubicin were consistent with previous reports using ionizing radiation (Kawamura et al., 2006; Sugihara et al., 2006; Saladino et al., 2009). However, we revealed that over half of cells had at least one pair of disengaged centrioles, something not previously reported. This led us to investigate why centrioles were not reduplicating despite becoming prematurely disengaged, which should "license" them to do so. We found that after DNA damage, activation of p53, and subsequently p21, led to inhibition of Cdk2 activity. Cdk2 activity is necessary for centriole duplication at the G1/S transition during the cell cycle (Hinchcliffe and Sluder, 2002). Consistent with these findings, p21 depletion leads to an increase in centrosome amplification in U2OS cells (Shimada et al., 2011). Interestingly, many transformed cell lines contain defects in the p53/p21 pathway. This provides an explanation for why many transformed cell lines display much more centrosome amplification after DNA damage than untransformed human cells. However, Cdk2 might not be the only protein that mediates centriole reduplication. For example, it was reported that DNA damage leads to p53-mediated downregulation of Plk4, a kinase required for daughter centriole assembly (Li et al., 2005; Nakamura et al., 2013). Thus, multiple levels of control might exist to limit centriole reduplication after DNA damage.

Moving forward, it would be interesting to see if inhibiting other proteins normally required for centriole duplication, such as Plk4 and SAS-6, would limit centriole reduplication in transformed cell lines. Reports have demonstrated that APC/C-Cdh1 activity targets SAS-6 for degradation in late anaphase (Strnad et al., 2007; Puklowski et al., 2011), and we, and others, have shown that APC/C is active after DNA damage. Thus, this would provide another explanation as to why only a small number of cells exhibit extra centrioles in untransformed cells. Consistent with this idea, we report that 97% of cells contain no SAS-6 staining at centrioles, by 48hrs after DNA damage.

DNA damage and centriole disengagement

We found that 52% of untransformed cells contained disengaged centrioles by 72hrs after treatment with Doxorubicin. Additionally, we demonstrated that either APC/C or Plk activities could disengage centrioles after DNA damage. These observations are consistent with the report that without DNA damage either Plk or APC/C activity alone is sufficient to disengage centrioles during prolonged S or G2 phases, albeit more slowly than both acting together (Hatano and Sluder, 2012; Loncarek et al., 2010; Prosser et al., 2012). However, many questions still remain. First, it is unclear which members of the Plk family actually participate in disengagement after damage. It is reported that Plk1, the obvious choice, is inhibited after DNA damage (Smits et al., 2000). Therefore, a few possible explanations exist. Plk1 activity could act early after

DNA damage to disengage centrioles and then becomes downregulated afterwards. To explore this, we attempted to stain cells for the phosphorylated active form of Plk1, which was shown to localize to centrioles in conditions that allow disengagement (Loncarek et al., 2010), at multiple time-points after DNA damage. However, we were unsuccessful at finding any localization at centrioles. Another option would be to repeat these experiments and quantify phosphorylated Plk1 levels by western blot analyses to determine if and when Plk1 becomes activated after DNA damage.

The second possibility is that Plk1 is not responsible for disengagement, but Plk2 or Plk3 can compensate for the activity. To support this idea, Plk2 and Plk3 activities were shown to rise after DNA damage (Bahassi, 2011). Further, according to unpublished results, Plk2 and Plk3 can phosphorylate the Plk1 target Emi1 in vitro (discussed in Wiebusch and Hagemeier, 2010). Our results using the Plk inhibitor BI 2536 could not distinguish between these possibilities because it inhibits the activities of Plk1, 2, and 3. Therefore, more specific inhibitors to Plk2 and Plk3 are needed in order to determine which proteins are responsible. Alternatively, RNAi of individual members could prove useful, but due to possible compensation caveats, this would have to be done very systematically.

The second major question that remains from our study is what are the targets of Plk and APC/C that lead to centriole disengagement? Reports show

that APC/C activity leads to the degradation of securin and subsequent activation of the protease Separase, which is required for centriole disengagement (Zou et al., 1999; Tsou and Stearns, 2006). However, the question still remains, what are Plk and Separase doing? There is attractive evidence that Plk1 and Separase regulate centriole disengagement in a similar fashion to sister chromatid separation. In prophase, Plk1 phosphorylates SA2, causing dissociation from chromosome arms, and it also phosphorylates Scc1, a cohesion subunit, causing it to be cleaved by Separase in late mitosis (Hauf et al., 2005; Peters et al., 2008). Recently, Schockel et al. (2011) demonstrated that expression of non-cleavable Scc1, blocked centriole disengagement, and conversely, cohesin subunits engineered to have cleavable sites promoted disengagement. In addition, many cohesion subunits are reported to localize to centrioles and control engagement (Thein et al., 2007; Wang et al., 2008; Nakamura et al., 2009; Beauchene et al., 2010; Gimenez-Abian et al., 2010). Thus, much evidence is growing to support the idea that centriole disengagement is regulated similarly to sister chromatid separation. While very appealing, many questions still remain. For example, does the entire cohesin complex or just a few subunits mediate engagement? Further, does the complex form a ring around centrioles as they do at chromosomes? With the advancements in super-resolution microscopy, it will be interesting and important to see if the localization pattern of some of these proteins can be determined at centrioles.

Centrosome amplification and cancer

For over 100 years it has been proposed that centrosomal defects can lead to aneuploidy and cancer (Boveri, 1914). During this time it has been shown that most tumors contain centrosome aberrations (reviewed in Nigg et al., 2014). Although the direct connection still remains unknown, it is proposed that the presence of extra centrosomes in mitosis leads to multipolar spindle formation or transient bipolar spindles, which can lead to lagging chromosomes, ultimately leading to genomic instability.

We demonstrated that after DNA damage, 10% of cells contain extra centrioles and 52% have disengaged centrioles. These, disengaged daughter centrioles displayed markers of maturation, suggesting they could assemble a spindle during mitosis. Thus, the total incidence of functional amplification was 62%. We were interested in knowing if cells containing disengaged or extra centrioles could enter into mitosis after DNA damage, and if so what was the consequence. We found that 14% of cells eventually entered mitosis after being prolonged in G2, and of these, 26% contained disengaged or extra centrioles. Interestingly, based on our time-lapse recordings, all cells that entered mitosis divided in a bipolar fashion. This suggests that the cells were able to cluster the centrosomes at mitosis to avoid multipolarity. This is not surprising as RPE1 cells commonly display centrosome clustering in the presence of extra centrosomes (Uetake and Sluder, 2004; Krzywicka-Racka and Sluder, 2011). However, even when cells form bipolar spindles with extra centrioles, often times

they go through a transient multipolar intermediate leading to lagging chromosomes (Ganem et al., 2009; Crasta et al., 2012). This suggests that DNA damage in normal proliferating cells could lead to genomic instability. This is especially troublesome for cancer patients who receive radiation therapy and/or DNA damaging drugs.

For future work, it would be of great importance to perform live-cell fluorescence imaging on RPE1 cells that progress into mitosis after DNA damage to determine if cells do experience lagging chromosomes. Further, it is unknown what happens to the daughter cells that formed from cells with extra centrosomes. Extension of time-lapse recordings might show if they immediately arrest in the next cell cycle or continue to proliferate. This could provide useful insight into whether cells can propagate with chromosome damage and/or genetic imbalances.

Phototoxicity in live-cell imaging

The light intensities used for fluorescence imaging can lead to photodamage and have toxic effects on living cells. Although this is a recognized problem for shorter wavelengths commonly used to visualize EGFP, the phototoxic effects of 546nm (green) light have not been systematically studied in mammalian cells. Therefore, we characterized the effects of 488nm and 546nm light on cell cycle progression in unlabeled untransformed human (hTERT-RPE1) cells. We chose these cells because they have an intact p53 pathway and stress

and/or damage is known to cause substantial delays or arrests in the cell cycle. This allowed us to use cell cycle progression as a marker for phototoxicity, which is a more sensitive assay than overt cell death. This is important because well before cells visually die from photodamage, they can experience altered cellular physiology, which can complicate experimental analysis without the knowledge of the researcher. Further, while primary RPE cells are pigmented, hTERT-RPE1 cells are not pigmented in culture (Rambhatla et al., 2002; Denton et al., 2006). Therefore, these cells should not contain additional light absorbing molecules and are a good representative of commonly used human cells in culture.

Effects of 488nm and 546nm light

In line with previous reports in different cell types, RPE1 cells were very sensitive to exposures of blue light (Zdolesk et al., 1990; Dixit and Cyr 2003; Hoebe et al., 2007; Robertson et al., 2013; Tinevez et al., 2013; Kuse et al., 2014). Single increasing irradiations led to a dose-dependent decrease in the percentage of cells that enter mitosis and cells that did reach mitosis took longer to do so. When we compared the effects of green (546nm) light to blue (488nm) light in both watts and total photons, we found that cells were much less sensitive to green light. Together, these findings demonstrate that shorter wavelengths of light are more harmful to untransformed human cells, which until now has only been an assumption. This suggests if only single color imaging is needed, using RFP constructs is a safer option for live-cell experiments. However, it is worth

noting that 546nm irradiations still led to a 10-15% decrease in cells that entered mitosis and thus, is not completely benign.

Interestingly, it is known that fluorescent proteins and dyes contribute to the generation of phototoxicity, but our results revealed that unlabeled RPE1 cells are intrinsically photosensitive. Thus, the question remains, what is leading to phototoxicity in these cells? While the answer is still up for debate there have been a few hypotheses in the literature. In 2009, it was shown that removing vitamins from cell culture media, specifically riboflavin, led to significant increases in the photostabilities of green fluorescent proteins (Bogdanov et al., 2009). The belief is that these vitamins can serve as cell permeant electron acceptors to propagate oxidative stress. Another, and not exclusive hypothesis, is that molecules in the cell can absorb light and promote the generation of photodamage. For example, mitochondria contain many molecules, such as cytochromes, flavoproteins, and NAD(P)H, that absorb both UV and visible light (Cheng and Packer, 1979). In support of this idea, it was demonstrated that non-UV visible light significantly impacts yeast metabolism, likely due to cytochrome light absorption (Robertson et al., 2013). In our experiments, the cell culture media was not devoid of vitamins, therefore, both scenarios are a possibility. However, if the phototoxic effects were due solely to molecules in the media, the effects should be widespread in the population since they would have to be diffusible. When we analyzed cells that were outside the irradiated area, they

were much healthier, suggesting that factors within the cells themselves are probably involved.

Impact of fluorescent proteins

Although our results revealed that unlabeled RPE1 cells are intrinsically photosensitive, it is possible that the amount of photodamage produced would be increased when fluorescent proteins are present. Indeed, Dixit and Cyr (2003) reported that the levels of reactive oxygen species (ROS) produced in tobacco cells that are expressing a fluorescent protein are increased compared to unlabeled cells. Our results demonstrated that RPE1 cells stably expressing GFP-centrin1 were more sensitive to blue light than unlabeled cells. Interestingly, control RPE1 mCherry-centrin1 cells displayed a longer average cell cycle length that unlabeled RPE1 cells. This result suggests that the presence of mCherry-centrin1 is a stress, which can increase the cell's sensitivity to further stressors, such as the mitotic shake-off. Despite this finding, when cells were irradiated with 546nm light we observed a dose dependent decrease in the percentage of cells that entered mitosis. Together these data provide evidence that excitation of fluorescent proteins can exacerbate the phototoxic effects of light on cells. In addition, the observations with mCherry-centrin1 cells indicate that even though green light exposure is relatively benign for cells, it is less so when it excites a fluorescent protein. Additionally, in our experiments we used fluorescently tagged centrin1, which is a cytosolic protein. For researchers

using cells expressing fluorescently tagged nuclear or mitochondrial proteins, there could be an increased risk of acquiring phototoxic effects due to their location. The generation of ROS in either of these organelles greatly increases the chances of inducing DNA damage and oxidative stress. Therefore, imaging conditions may need to be further adjusted depending on the tagged protein of interest.

Moving forward, as the generation and improvements of far-red exciting fluorescent proteins continues, it will be interesting to see if phototoxicity can be further alleviated with the use of even longer wavelengths of light. This may allow researchers who require multicolor imaging to shift to the combination of RFPs and far-red exciting proteins. Further, multi-photon microscopy, which utilizes light in the far-red, may be a safer option for live-cell imaging.

Reciprocity relationships

It is commonly believed that the rate at which photons are delivered to cells impacts the level of phototoxicity produced (discussed in Magidson and Khodjakov, 2013). For example, long exposures with low intensity light are thought to be less harmful to cells than short exposures using high intensity light. The belief is that spreading the total dose over a longer period of time allows for cells to appropriately scavenge excess ROS or repair a certain amount of photodamage. Only when the damage reaches a certain threshold does it pose a problem to cells. For tobacco cells, Dixit and Cyr (2003) reported that reducing

blue light intensity, but increasing exposure times resulted in less mitotic arrest and cell death, despite a higher total energy dose.

We tested this hypothesis in two different fashions. First, we spread our single irradiations into 10s pulses, administered every minute until the total exposures were the same and secondly, we added a neutral density filter, allowing only 10% transmission of light, and extending our irradiation times ten-fold. Our results, however, revealed no consistent improvements in cell cycle progression for either condition. Therefore, for untransformed human cells, if the total energy dose is constant, the rate at which the photons are delivered does not have an impact on the phototoxic effects on cell cycle progression. This suggests that sacrificing signal to noise to improve cell health may not always be necessary. However, this may also vary depending on the imaging system used. For example, with confocal microscopy, each point in the sample receives short, high intense pulses of light as opposed to continuous sample illumination for wide-field microscopy. With such high powered and directed pulses, the risk of severely damaging cells increases. Indeed, Tinevez et al., (2012) reported that for the same total energy dose administered to *C. elegans* embryos, spinning-disk confocal microscopy induced more photodamage than wide-field microscopy. Therefore, reducing light intensity and extending exposures might be required for live-cell imaging in other systems. None-the-less, for all applications it is important to find the appropriate balance between exposure time and light intensity to avoid phototoxicity that could confound results.

Oxidative stress

We have shown that blue light is extremely damaging to untransformed human cells. Although cells tolerated green light much better than blue light, imaging with the use of only RFP's is not always an option. Often times the signal is not bright enough, or simply multiple colors are desired. Since the generation of reactive oxygen species is believed to be the driving force in the production of photodamage (Zdolesk et al., 1993; Dixit and Cyr, 2003), we were interested if reducing the level of oxidative stress may allow cells to cope with and relieve photodamage before it becomes a burden. Indeed, the use of oxygen scavengers has shown to reduce photobleaching during live-cell fluorescence imaging (reviewed in Waters, 2013). Our results revealed that culturing cells at oxygen levels closer to physiological conditions (~3%) or the addition of Trolox, a water-soluble antioxidant, to the cell culture media, significantly improved cell cycle progression after exposure to blue light. While both treatments were successful, the addition of Trolox showed greater improvements. Remarkably, ~40% more cells treated with Trolox entered mitosis after the 1min single irradiations of blue light compared to cells without Trolox treatment. Further, cell cycle timing for these cells was very similar to that of control shake-off cells, suggesting an almost entirely healthy population. These findings provide researchers an easy and effective method of reducing phototoxicity for long-term live-cell fluorescence imaging.

BIBLIOGRAPHY

Anderhub SJ, Kramer A, Maier B. 2012. Centrosome amplification in tumorigenesis. Cancer Lett 322:8-17.

Bahassi EM. 2011. Polo-like kinases and DNA damage checkpoint: beyond the traditional mitotic functions. Exp Biol Med (Maywood) 236:648-57.

Balczon R, Bao L, Zimmer WE, Brown K, Zinkowski RP, Brinkley BR. 1995. Dissociation of centrosome replication events from cycles of DNA synthesis and mitotic division in hydroxyurea-arrested Chinese hamster ovary cells. J Cell Biol 130:105–15

Basto R, Brunk K, Vinadogrova T, Peel N, Franz A, Khodjakov A, Raff JW. 2008. Centrosome amplification can initiate tumorigenesis in flies. Cell 133:1032-42.

Beauchene NA, Diaz-Martinez LA, Furniss K, Hsu WS, Tsai HJ, Chamberlain C, Esponda P, Gimenez-Abian JF, Clarke DJ. 2010. Rad21 is required for centrosome integrity in human cells independently of its role in chromosome cohesion. Cell Cycle 9:1774-1780

Bogdanov AM, Bogdanova EA, Chudakov DM, Gorodnicheva TV, Lukyanov S, Lukyanov KA. 2009. Cell culture medium affects GFP photostability: a solution. Nat Methods 6:859-60.

Bourke E, Dodson H, Merdes A, Cuffe L, Zachos G, Walker M, Gillespie D, Morrison CG. 2007. DNA damage induces Chk1-dependent centrosome amplification. EMBO Rep 8:603-9.

Bourke E, Brown JAL, Takeda S, Hochegger H, Morrison CG. 2010. DNA damage induces Chk1-dependent threonine-160 phosphorylation and activation of Cdk2. Oncogene 29:616-24.

Boveri T. 1914. The Origin of Malignant Tumors, Williams and Wilkins, Baltimore, MD.

Brinkley BR. 2001. Managing the centrosome numbers game: from chaos to stability in cancer cell division. Trends Cell Biol 11:18-21.

Cardullo RA. 2013.Theoretical principles and practical considerations for fluorescence resonance energy transfer microscopy. Methods Cell Biol 114: 441-56.

Carlton PM, Boulanger J, Kervrann C, Sibarita JB, Salamero J, Gordon-Messer S, Bressan D, Haber JE, Haase S, Shao L, Winoto L, Matsuda A, Kner P, Uzawa S, Gustafsson M, Kam Z, Agard DA, Sedat JW. 2010. Fast live simultaneous multiwavelength four-dimensional optical microscopy. Proc Natl Acad Sci USA 107:16016-22.

Chen LC, Lloyd WR, Chang CW, Sud D, Mycek MA. 2013. Fluorescence lifetime imaging microscopy for quantitative biological imaging. Methods Cell Biol 114:457-88.

Cheng LY, Packer L.1979 Photodamage to hepatocytes by visible light. FEBS Lett 97:124–8.

Cheung-Ong K, Giaever G, Nislow C. 2013. DNA-damaging agents in cancer chemotherapy: serendipity and chemical biology. Chem Biol 20:648-59.

Chiba S, Okuda M, Mussman JG and Fukasawa K. 2000. Genomic convergence and suppression of centrosome hyperamplification in primary $p53^{-/-}$ cells in prolonged culture. Exp. Cell Res 258:310–321.

Cimini D, Howell B, Maddox P, Khodjakov A, Degrassi F, Salmon ED. 2001. Merotelic kinetochore orientation is a major mechanism of aneuploidy in mitotic mammalian tissue cells. J Cell Biol 153:517-27.

Conroy PC, Saladino C, Dantas TJ, Lalor P, Dockery P, Morrison CG. 2012. C-NAP1 and rootletin restrain DNA damage-induced centriole splitting and facilitate ciliogenesis. Cell Cycle 11:3769-78.

Crasta K, Surana U. 2006. Disjunction of conjoined twins: Cdk1, Cdh1 and separation of centrosomes. Cell division 1:12.

Crasta K, Ganem NJ, Dagher R, Lantermann AB, Ivanova EV, Pan Y, Nezi L, Protopopov A, Chowdhury D, Pellman D. 2012. DNA breaks and chromosome pulverization from errors in mitosis. Nature 482:53-8.

Dammermann A, Maddox PS, Desai A, Oegema K. 2008. SAS-4 is recruited to a dynamic structure in newly forming centrioles that is stabilized by the gamma-tubulin-mediated addition of centriolar microtubules. J Cell Biol 180:771-85.

D'Assoro AB, Lingle WL, Salisbury JL. 2002. Centrosome amplification and the development of cancer. Oncogene 21:6146-53.

Denton ML, Foltz MS, Estlack LE, Stolarski DJ, Noojin GD, Thomas RJ, Eikum D, Rockwell BA. 2006. Damage Thresholds for Exposure to NIR and Blue Lasers in an In Vitro RPE Cell System. Invest Ophthalmol Vis Sci 47:3065-73

Dixit R, Cyr R. 2003. Cell damage and reactive oxygen species production induced by fluorescence microscopy: effect on mitosis and guidelines for non-invasive fluorescence microscopy. Plant J 36:280-90.

Dodson H, Bourke E, Jeffers LJ, Vagnarelli P, Sonoda E, Takeda S, Earnshaw WC, Merdes A, Morrison C. 2004. Centrosome amplification induced by DNA damage occurs during a prolonged G2 phase and involves ATM. EMBO J 23:3864-73.

Dynlacht BD, Khodjakov A., and Gonczy P. (2009). Overly long centrioles and defective cell division upon excess of the SAS-4-related protein CPAP. Curr. Biol. 19:1012–1018.

Fukasawa K, Choi T, Kuriyama R, Rulong, S, Vande Woude GF. 1996. Abnormal centrosome amplification in the absence of p53. Science 271:1744-1747.

Fukasawa K. 2007. Oncogenes and tumour suppressors take on centrosomes. Nat Rev Cancer 7:911-24.

Ganem NJ, Godinho SA, Pellman D. 2009. A mechanism linking extra centrosomes to chromosomal instability. Nature 460:278-82.

Gard DL, Hafezi S, Zhang T, Doxsy SJ. 1990. Centrosome duplication continues in cycloheximide-treated Xenopus blastulae in the absence of a detectable cell cycle. J Cell Biol 110:2033-42.

Giménez-Abián JF, Diaz-Martinez LA, Beauchene NA, Hsu WS, Tsai HJ, Clarke DJ. 2010. Determinants of Rad21 localization at the centrosome in human cells. Cell Cycle 9:1759-63.

Godinho SA, Kwon M, Pellman D. 2009. Centrosomes and cancer: how cancer cells divide with too many centrosomes. Cancer Metastasis Rev 28:85-98.

Goepfert TM, Adigun YE, Zhong L, Gay J, Medina D, Brinkley WR. 2002. Centrosome amplification and overexpression of aurora A are early events in rat mammary carcinogenesis. Cancer Res 62:4115-22.

Ham WT Jr., Ruffolo JJ Jr., Mueller HA, Guerry D III. 1980. The nature of retinal radiation damage: dependence on wavelength, power level and exposure time;

the quantitative dimensions of intense light damage as obtained from animal studies, Section II. Applied Research, 20, 1005-1111.

Hanashiro K, Kanai M, Geng Y, Sicinski P, Fukasawa K. 2008. Roles of cyclins A and E in induction of centrosome amplification in p53-compromised cells. Oncogene 27:5288-302.

Hansen DV, Loktev A, Ban KH, Jackson PK. 2004. Plk1 regulates activation of the anaphase promoting complex by phosphorylating and triggering SCFbetaTrCP-dependent destruction of the APC Inhibitor Emi1. Mol Biol Cell 15:5623-34.

Hatano T, Sluder G. 2012. The interrelationship between APC/C and Plk1 activities in centriole disengagement. Biol Open 1:1153-60.

Hauf S, Roitinger E, Koch B, Dittrich CM, Mechtler K, Peters, JM. 2005. Dissociation of cohesin from chromosome arms and loss of arm cohesion during early mitosis depends on phosphorylation of SA2. PLoS Biol. 3:e69.

Hinchcliffe EH and Sluder G. 2001."It takes two to tango": understanding how centrosome duplication is regulated throughout the cell cycle. Genes Dev 15:1167-81

Hinchcliffe EH, Sluder G. 2002. Two for two: Cdk2 and its role in centrosome doubling. Oncogene 21:6154-60.

Hoebe RA, Van Oven CH, Gadella TWJ, Dhonukshe PB, Van Noorden JF, Manders EMM. 2007. Controlled light-exposure microscopy reduces photobleaching and phototoxicity in fluorescence live-cell imaging. Nat Biotechnol 25:249-53.

Hornick JE, Mader CC, Tribble EK, Bagne CC, Vaughan KT, Shaw SL, Hinchcliffe EH. 2011. Amphiastral mitotic spindle assembly in vertebrate cells lacking centrosomes. Curr Biol 21:598-605

Hyun SY, Hwang HI, Hwan HI, Jang YJ. Polo-like kinase-1 in DNA damage response. 2014. BMB Rep 47:249-55.

Inanç B, Dodson H, Morrison CG. 2010 A centrosome-autonomous signal that involves centriole disengagement permits centrosome duplication in G2 phase after DNA damage. Mol Biol Cell 21:3866-77.

Kawamura K, Fujikawa-Yamamoto K, Ozaki M, Iwabuchi K, Nakashima H, Domiki C, Morita N, Inoue M, Tokunaga K, Shiba N, Ikeda R, Suzuki K. 2004. Centrosome hyperamplification and chromosomal damage after exposure to radiation. Oncology 67:460-70.

Kawamura K, Morita N, Domiki C, Fujikawa-Yamamoto K, Hashimoto M, Iwabuchi K, Suzuki K. 2006. Induction of centrosome amplification in p53 siRNA-treated human fibroblast cells by radiation exposure. Cancer Sci 97:252-8.

Khodjakov A and Rieder CL. 1999. The sudden recruitment of gamma-tubulin to the centrosome at the onset of mitosis and its dynamic exchange throughout the cell cycle, do not require microtubules. J Cell Biol 146:585-96.

Khodjakov A and Rieder CL. 2001. Centrosomes enhance the fidelity of cytokinesis in vertebrates and are required for cell cycle progression. J Cell Biol 153:237-42.

Khodjakov A, Rieder CL, Sluder G, Casseis G, Sibon O, Wang CL. 2002. De novo formation of centrosomes in vertebrate cells arrested during S phase. J Cell Biol 158:1171-81.

Kleylein-Sohn J, Westerndorf J, Clech ML, Habedanck R, Stierhof YD, Nigg EA. 2007. Plk4-induced centriole biogenesis in human cells. Dev Cell 13:190-202.
Kohlmaier, G, Loncarek, J, Meng X, McEwen BF, Mogensen MM, Spektor A,

Krämer A, Neben K, Ho AD. 2002. Centrosome replication, genomic instability and cancer. Leukemia 16:767-75.

Krishnan B, Morgan GJ. 2007. Non-Hodgkin lymphoma secondary to cancer chemotherapy. Cancer Epidemiol Biomarkers Prev 16:377-80.

Krzywicka-Racka A, Sluder G. 2011. Repeated cleavage failure does not establish centrosome amplification in untransformed human cells. J Cell Biol 194:199-207.

La Terra S, English CN, Hergert P, McEwen BF, Sluder G, Khodjakov A. 2005. The de novo centriole assembly pathway in HeLa cells: cell cycle progression and centriole assembly/maturation. J Cell Biol 168:713–22

Lee K, Rhee K. 2012. Separase-dependent cleavage of pericentrin B is necessary and sufficient for centriole disengagement during mitosis. Cell Cycle 11:2476-85.

Lengauer C, Kinzler KW, Vogelstein B. 1998. Genetic instabilities in human cancers. Nature 396:643-9.

Li J, Tan M, Li L, Pamarthy D, Lawrence TS, Sun Y. 2005. SAK, a new polo-like kinase, is transcriptionally repressed by p53 and induces apoptosis upon RNAi silencing. Neoplasia 7:312-23.

Lingle WL, Salisbury JL. 2000. The role of the centrosome in the development of malignant tumors. Curr Top Dev Biol 49:313-29.

Lingle WL, Barrett SL, Negron VC, D'Assoro AB, Boeneman K, Liu W, Whitehead CM, Reynolds C, Salisbury JL. 2002. Centrosome amplification drives chromosomal instability in breast tumor development. Proc Natl Acad Sci USA 99:1978-83.

Löffler H, Fetcher A, Liu FY, Poppelreuther S, Krämer A. 2012. DNA damage-induced centrosome amplification occurs via excessive formation of centriolar satellites. Oncogene 32:2963-72.

Loncarek J, Hergert P, Magidon V, Khodjakov A . Control of daughter centriole formation by the pericentriolar material. 2008.Nat Cell Biol 10:322-8.

Loncarek J and Khodjakov A. 2009 Ab ovo or de novo? Mechanisms of centriole duplication. Mol Cells 27:135-42.

Lončarek J, Hergert P, Khodjakov A. 2010. Centriole Reduplication during Prolonged Interphase Requires Procentriole Maturation Governed by Plk1. Curr Biol 20:1277-1282.

Magidson V, Khodjakov A. 2013. Circumventing photodamage in live-cell microscopy. Methods Cell Biol 114:545-60.

Marshall, WF, Vucica Y, and Rosenbaum, JL. 2001. Kinetics and regulations of de novo centriole assembly: implications for the mechanism of centriole duplication. Curr. Biol. 11:308–317,

Matsuo K, Ohsumi K, Iwabuchi M, Kawamata T, Ono Y, Takahashi M. 2012. Kendrin Is a Novel Substrate for Separase Involved in the Licensing of Centriole Duplication. Curr Biol 22:915-21.

Maugeri-Saccà M, Bartucci M, Maria RD. 2013. Checkpoint kinase 1 inhibitors for potentiating systemic anticancer therapy. Cancer Treat Rev 39:525-33.

Moshe Y, Boulaire J, Pagano M, Hershko A. 2004. Role of Polo-like kinase in the degradation of early mitotic inhibitor 1, a regulator of the anaphase promoting complex/cyclosome. Proc Natl Acad Sci USA 101:7937-42.

Nakamura A, Arai H, Fujita N. 2009. Centrosomal Aki1 and cohesin function in separase-regulated centriole disengagement. J Cell Biol 187:607-14.

Nakamura T, Saito H, Takekawa M. 2013. SAPK pathways and p53 cooperatively regulate PLK4 activity and centrosome integrity under stress. Nat Commun 4:1775.

Nigg EA. 2002. Centrosome aberrations: cause or consequence of cancer progression? Nat Rev Cancer 2:815-25.

Nigg EA, Stearns T. 2011. The centrosome cycle: Centriole biogenesis, duplication and inherent asymmetries. Nat Cell Biol 13:1154-60.

Nigg EA, Cajanek L, Arquint C. 2014. The centrosome duplication cycle in health and disease. FEBS Lett 588:2366-72.

O'Connor N, Silver RB. 2013. Ratio imaging: practical considerations for measuring intracellular Ca2+ and pH in living cells. Methods Cell Biol 114:387-406.

Orr-Weaver TL, Weinberg RA. 1998. A checkpoint on the road to cancer. Nature 392:223-4.

Peters JM, Tedeschi, A, Schmitz J. 2008. The cohesin complex and its roles in chromosome biology. Genes Dev 22:3089-3114.

Piel M, Nordberg J, Euteneuer U, Bornens M. 2001. Centrosome-dependent exit of cytokinesis in animal cells. Science 291:1550-3.

Pihan GA, Purohit A, Wallace J, Malhotra R, Liotta L, Doxsey SJ. 2001. Centrosome defects can account for cellular and genetic changes that characterize prostate cancer progression. Cancer Res 61:2212-9.

Pihan GA, Wallace J, Zhou Y, Doxsey SJ. 2003. Centrosome abnormalities and chromosome instability occur together in pre-invasive carcinomas. Cancer Res 63:1398-404.

Prosser SL, Samant MD, Baxter JE, Morrison CG, Fry AM. 2012. Oscillation of APC/C activity during cell cycle arrest promotes centrosome amplification. J Cell Sci 125:5353-68.

Puklowski A, Homsi Y, Keller D, May M, Chauhan S, Kossatz U, Grunwald V, Kubicka S, Pich A, Manns MP, Hoffmann I, Gonczy P, Malek N. 2011. The SCF-FBXW5 E3-ubiquitin ligase is regulated by PLK4 and targets HsSAS-6 to control centrosome duplication. Nat Cell Biol 13:1004-9.

Rambhatla L, Chiu CP, Glickman RD, Rowe-Rendleman C. 2002. In vitro differentiation capacity of telomerase immortalized human RPE cells. Invest Ophthalmol Vis Sci 43:1622-30.

Robertson JB, Davis CR, Johnson CH. 2013. Visible light alters yeast metabolic rhythms by inhibiting respiration. Proc Natl Acad Sci USA 110:21130-5.

Rodrigues-Martins A, Bettencourt-Dias M, Riparbelli M, Ferreira C, Ferreira I, Callaini G, Glover DM. 2007. DSAS-6 organizes a tube-like centriole precursor, and its absence suggests modularity in centriole assembly. Curr Biol 17:1465-72.

Saladino C, Bourke E, Conroy PC, Morrison CG. 2009. Centriole separation in DNA damage-induced centrosome amplification. Environ Mol Mutagen 50:725-32.

Sato N, Mizumoto K, Nakamura M, Tanaka M. 2000. Radiation-induced centrosome overduplication and multiple mitotic spindles in human tumor cells. Exp Cell Res 255:321-6.

Schöckel L, Mockel M, Mayer B, Boos D, Stemmann O. 2011. Cleavage of cohesin rings coordinates the separation of centrioles and chromatids. Nat Cell Biol

Sen CK, Roy S. 2010. Oxygenation state as a driver of myofibroblast differentiation and wound contraction: hypoxia impairs wound closure. J Invest Dermatol 130:2701-3.

Shimada M, Komatsu K. 2009. Emerging connection between centrosome and DNA repair machinery. J Radiat Res 50:295-301.

Shimada M, Kobayashi J, Hirayama R, Komatsu K. 2010. Differential role of repair proteins, BRCA1/NBS1 and Ku70/DNA-PKcs, in radiation-induced centrosome overduplication. Cancer Sci 101:2531-7.

Shimada M, Kato A, Habu T, Komatsu K. 2011. Genistein, isoflavonoids in soybeans, prevents the formation of excess radiation-induced centrosomes via p21 up-regulation. Mutation research 716:27-32.

Sluder G, Rieder CL. 1985. Centriole number and the reproductive capacity of spindle poles. J Cell Biol 100:887-96.

Sluder G, Miller FJ, Cole R, Rieder CL. 1990. Protein synthesis and the cell cycle: centrosome reproduction in sea urchin eggs is not under translational control. J Cell Biol 110:2025-32.

Sluder, G. 2004. Centrosome Duplication and its Regulation in the Higher Animal Cell. In Centrosomes in Development and Disease. E. Nigg editor. Wiley VCH/Weinheim. 167-189.

Sluder G, Khodjakov A. 2010. Centriole duplication: analogue control in a digital age. Cell Biol Int 34:1239-45.

Smits VA, Klompmaker R, Arnaud L, Rijksen G, Nigg EA, Medema RH. 2000. Polo-like kinase-1 is a target of the DNA damage checkpoint. Nat Cell Biol 2:672-6.

Steegmaier M, Hoffman M, Baum A, Lénárt P, Petronczki M, Krssák M, Gürtler U, Garin-Chesa P, Lieb S, Quant J, Grauert M, Adolf G, Kraut N, Peters JM, Rettig W. 2007. BI 2536, a potent and selective inhibitor of polo-like kinase 1, inhibits tumor growth in vivo. Curr Biol 17:316-22.

Stephens D, Allan VJ. 2003. Light microscopy techniques for live cell imaging. Science 300:82-6.

Strnad P, Leidel S, Vinogradova T, Euteneuer U, Khodjakov A, Gonczy P. 2007. Regulated HsSAS-6 levels ensure formation of a single procentriole per centriole during the centrosome duplication cycle. Dev Cell 13:203-13.

Stucke VM, Sillje HH, Arnaud L, Nigg EA. 2002. Human Mps1 kinase is required for the spindle assembly checkpoint but not for centrosome duplication. EMBO J 21:1723–32.

Sugihara E, Kanai M, Saito S, Nitta T, Toyoshima H, Nakayama K, Nakamaya KI, Fukasawa K, Schwab M, Saya H, Miwa M. 2006. Suppression of centrosome amplification after DNA damage depends on p27 accumulation. Cancer Res 66:4020-9.

Swedlow, JR, Andrews, PD. 2005. In vivo imaging of mammalian cells. Live cell imaging: A laboratory manual. CSHL Press, Cold Spring Harbor pp. 329–343.

Szollosi D, Calarco P, and Donahue RP. 1972. Absence of centrioles in the first and second meiotic spindles of mouse oocytes. J. Cell Sci 11:521–541.

Tarapore P, Fukasawa K. 2002. Loss of p53 and centrosome hyperamplification. Oncogene 21:6234-40.

Thein KH, Kleylein-Sohn J, Nigg EA, Gruneberg U. 2007. Astrin is required for the maintenance of sister chromatid cohesion and centrosome integrity. J Cell Biol 178:345-54.

Tsou MF, Stearns T. 2006. Mechanism limiting centrosome duplication to once per cell cycle. Nature 442:947-51.
Tsou MF, Wang WJ, George KA, Uryu K, Stearns T, Jallepalli PV. 2009. Polo kinase and separase regulate the mitotic licensing of centriole duplication in human cells. Dev Cell 17:344-54.

Uetake Y, Sluder G. 2004. Cell cycle progression after cleavage failure: mammalian somatic cells do not possess a "tetraploidy checkpoint". J Cell Biol 165:609-15.

Uetake Y, Loncarek J, Nordberg JJ, English CN, La Terra S, Khodjakov A, Sluder G. 2007. Cell cycle progression and de novo centriole assembly after centrosomal removal in untransformed human cells. J Cell Biol 176:173-82.

Uetake Y, Sluder G. 2010. Prolonged prometaphase blocks daughter cell proliferation despite normal completion of mitosis. Curr Biol 20:1666-71.

Uetake Y, Sluder G. 2012. Practical Methodology for Long-Term Recordings of Live Human Cells. In: Shaked NT, Zalevsky Z, Satterwhite L, editors. Biomedical Optical Phase Microscopy and Nanoscopy. Academic Press. p 43–52.

Varmark H, Sparks CA, Nordberg JJ, Koppetsch BS, Theurkauf WE. 2009. DNA damage-induced cell death is enhanced by progression through mitosis. Cell Cycle 8:2951-63.

Wang X, Yang Y, Duan Q, Jiang N, Huang Y, Darzynkiewicz Z, . 2008. sSgo1, a major splice variant of Sgo1, functions in centriole cohesion where it is regulated by Plk1. Dev Cell 14:331-41.

Wang WJ, Soni RK, Uryu K, Tsou MF. 2011. The conversion of centrioles to centrosomes: essential coupling of duplication with segregation. J Cell Biol 193:727-39.

Waters J. 2013. Live-cell fluorescence imaging. Methods Cell Biol 114:125-50

Weaver BA, Silk AD, Montagna C, Verdier-Pinard P, Cleveland DW. 2007. Aneuploidy acts both oncogenically and as a tumor suppressor. Cancer Cell 11:25-36.

Wiebusch L, Hagemeier C. 2010. p53- and p21-dependent premature APC/C-Cdh1 activation in G2 is part of the long-term response to genotoxic stress. Oncogene 29:3477-89.

Zdolsek JM, Olsson GM, Brunk UT. 1990. Photooxidative damage to lysosomes of cultured macrophages by acridine orange. Photochem Photobiol 51:67-76.

Zdolsek JM. 1993. Acridine orange-mediated photodamage to cultured cells. APMIS 101:127-32.

Zhou BB, Elledge SJ. 2000. The DNA damage response: putting checkpoints in perspective. Nature 408:433-9.

Zou H, McGarry TJ, Bernal T, Kirschner MW. 1999. Identification of a vertebrate sister-chromatid separation inhibitor involved in transformation and tumorigenesis. Science 285:418-22.